# NATIONAL ADVISORY COMMITTEE FOR AERONAUTICS

**TECHNICAL NOTE 3623**

# CORRELATION OF SUPERSONIC CONVECTIVE HEAT-TRANSFER COEFFICIENTS FROM MEASUREMENTS OF THE SKIN TEMPERATURE OF A PARABOLIC BODY OF REVOLUTION (NACA RM-10)

By Leo T. Chauvin and Carlos A. deMoraes

Langley Aeronautical Laboratory
Langley Field, Va.

Washington
March 1956

1P

NATIONAL ADVISORY COMMITTEE FOR AERONAUTICS

TECHNICAL NOTE 3623

# CORRELATION OF SUPERSONIC CONVECTIVE HEAT-TRANSFER COEFFICIENTS FROM MEASUREMENTS OF THE SKIN TEMPERATURE OF A PARABOLIC BODY OF REVOLUTION (NACA RM-10)[1]

By Leo T. Chauvin and Carlos A. deMoraes

## SUMMARY

Local coefficients of convective heat transfer have been evaluated from skin temperatures measured along the body of an NACA research missile designated the RM-10. The general shape of the body was a parabola of revolution of fineness ratio 12.2. Heat-transfer data are presented for a Mach number range of 1.02 to 2.48 and for a Reynolds number range of $3.18 \times 10^6$ to $163.85 \times 10^6$ based on the axial distance from the nose to the point at which temperature measurements were made.

Results from the data obtained are presented as the product of Nusselt number $N_{Nu}$ and the -1/3 power of Prandtl number $N_{Pr}$ against Reynolds number R based on axial distance to the station where the measurements were made. The equation for heat transfer for a turbulent boundary layer on a flat plate in subsonic flow $\left(N_{Nu}N_{Pr}^{-1/3} = 0.0296\ R^{0.8}\right)$ is shown to be in good agreement with the test results when the heat-transfer parameters are based on the temperature just outside the boundary layer. Basing the correlation of heat-transfer parameters on air properties calculated at the wall temperature gave results that were in good agreement with the equation for convective heat transfer for cones in a supersonic flow $N_{Nu}N_{Pr}^{-1/3} = 0.034\ R^{0.8}$. Heat-transfer coefficients from the V-2 tests correlated on a Nusselt, Prandtl, and Reynolds number relation gave values that were approximately 15 percent lower than the results obtained on the RM-10 research missile, for conditions where the parameters were based on the temperature just outside the boundary layer, or on the wall temperature. Values of recovery factor were obtained for the stations at which temperature measurements were made and are in agreement with theoretical values of recovery factors for a flat plate.

---

[1]Supersedes declassified NACA Research Memorandum L51A18 by Leo T. Chauvin and Carlos A. deMoraes, 1951.

## INTRODUCTION

Aerodynamic heating in supersonic flight has long been recognized as a major problem in the design of supersonic aircraft, and experimental heat-transfer data for high Mach numbers and Reynolds numbers are in great demand. Except for some work done on the V-2, all of the convective heat-transfer work has been done in wind tunnels utilizing steady-state conditions; however, the results presented herein are for the transient conditions encountered along the trajectory.

Inasmuch as the problem of aerodynamic heating is closely related with that of skin-friction drag, investigations of these two phenomena are being carried out simultaneously by the Langley Pilotless Aircraft Research Division as a part of an NACA program on supersonic aerodynamics. Models of a specific configuration, designated NACA RM-10, were flight-tested at the Pilotless Aircraft Research Station at Wallops Island, Va.

Heat-transfer coefficients obtained from data measured on two RM-10 test vehicles are presented herein. The transient conditions encountered during the flight of a rocket-propelled test vehicle are particularly suited for obtaining aerodynamic heating and heat-transfer data. The skin temperature measured along the body by resistance-type thermometers cemented to the inner surface of the skin was continuously telemetered to a ground receiving station during the time of flight. From these data the skin temperature, time rate of change of skin temperature, adiabatic wall temperature, and convective heat-transfer coefficient were determined.

The Mach number range covered in these tests was approximately 1.0 to 2.5. The Reynolds number range, based on free-stream conditions and distance along the axis of the missile from the nose to the test station, was approximately $3.18 \times 10^6$ to $163.85 \times 10^6$.

## SYMBOLS

| | |
|---|---|
| $A$ | area, sq ft |
| $C_p$ | specific heat of air, Btu/slug/$^\circ$F |
| $C_w$ | specific heat of wall, Btu/lb/$^\circ$F |
| $h_e$ | local effective convective heat-transfer coefficient, Btu/(sec)(sq ft)($^\circ$F) |

| | |
|---|---|
| $k$ | thermal conductivity of air, Btu/(sec)(sq ft)($^{\circ}$F/ft) |
| $l$ | distance from the nose along the axis of the body, ft |
| $N_{Nu}$ | Nusselt number, $h_e l/k$, dimensionless |
| $N_{Pr}$ | Prandtl number, $C_p\mu/k$, dimensionless |
| $Q$ | quantity of heat, Btu |
| $R$ | Reynolds number, $\rho V l/\mu$, dimensionless |
| RF | recovery factor |
| $T$ | temperature, $^{\circ}$F or $^{\circ}$R |
| $t$ | time from start of flight, sec |
| $V$ | velocity, ft/sec |
| $\gamma_w$ | specific weight of wall, lb/cu ft |
| $\mu$ | viscosity of air, slugs/ft-sec |
| $\rho$ | density of air, slugs/cu ft |
| $\tau$ | thickness, ft |

Subscripts:

| | |
|---|---|
| aw | adiabatic wall |
| w | conditions of material pertaining to wall |
| o | undisturbed free stream ahead of model |
| s | isentropic stagnation |
| v | just outside boundary layer |

## TEST VEHICLES

The general configuration and body equation of the RM-10 are shown in figure 1. Figure 2 is a photograph of the test vehicle on the launcher. The bodies were basically parabolas of revolution having a maximum diameter

of 12 inches and a fineness ratio of 15; however, the stern was cut off at 81.3 percent of full length to allow for the installation of the rocket motor. This decrease in length resulted in an actual fineness ratio of 12.2. Four untapered stabilizing fins were equally spaced around the afterbody. They were swept back 60° with a total aspect ratio of 2.04 and had a 10-percent-thick circular-arc cross section normal to the leading edge. The design was chosen to attain a high degree of stability which insured testing at zero angle of attack.

The RM-10 test vehicles were designed for heat-transfer investigations covering large Mach number and Reynolds number ranges. A minimum of internal structure was accomplished by internally pressurizing the models. Figure 3 shows the internal construction of the models.

The test vehicles were all metal in construction, utilizing spun magnesium alloy skins and cast magnesium alloy tail sections to which the fins were welded. The skin thickness used for each station is tabulated in table I. All the surfaces were smooth and highly polished at the time of flight.

Both models were propelled by a 6.25-inch ABL Deacon rocket motor carried internally. The case of the rocket motor has a temperature rise of 50° F which was not sufficient to affect the accuracy of the tests. This small rise in temperature is due to the internal burning of a Deacon rocket motor; that is, the burning starts in the center and works outward toward the case so that the powder and the inhibitor act as insulators between the flame and the rocket case.

## INSTRUMENTATION AND TESTS

Skin temperatures were measured by means of resistance-type thermometers cemented to the inner surface of the skin. These thermometers were made of fine platinum wire 0.0002 inch in diameter. Reference 1 describes the thermometers more completely.

Thermometers were located at stations 8.9, 17.8, 36.2, 49.9, 86.1, and 123.5 on one test vehicle (model A) and at stations 14.3, 18.3, and 85.3 on the other test vehicle (model B). Reference 1 shows that these thermometers had a time lag of 3 milliseconds, corresponding to a maximum temperature error of 0.3° F for the test conditions where the heat transfer is the greatest. This error was considered to be negligible compared with the 3.2° F error due to the thickness of the skin. Continuous temperature readings were telemetered to ground receiving stations.

The models were launched from a zero-length launcher at an elevation angle of 55°. Data were obtained during the decelerating portion of the

flight trajectory. Trajectory and atmospheric data were obtained from the NACA modified SCR 584 radar theodolite and by radiosonde observations. The time history of the flight velocity was obtained from the continuous-wave Doppler theodolite radar unit (as described in ref. 2). Thermodynamic properties of the air shown in figure 4 were obtained from reference 3. The specific heat of the magnesium wall presented in figure 5 was obtained from reference 4.

Time histories of the measured skin temperature presented in figure 6 were obtained as the vehicles coasted from a Mach number of approximately 2.5 to 1.0. At the time of rocket motor burnout, which was approximately 3.2 seconds after the start of flight, the test vehicles were at their maximum velocity and Mach number. No skin temperature measurements were obtained throughout the initial 3.2 seconds, the period of powered flight, during which time the telemeter signal was unsatisfactory. Properties of the air in the undisturbed free stream ahead of the models and Mach number for models A and B are shown in figure 7 plotted against time. Reynolds number per foot, based on free-stream conditions, is shown in figure 8 plotted against Mach number. The difference in Reynolds number between the two models is attributed to differences in atmospheric conditions and performance of the rocket motors.

## METHODS AND PROCEDURES

The transient conditions encountered during the flight of the rocket-powered test vehicle result in a heating of the skin by the boundary layer during the first part of the flight and a cooling of the skin by the boundary layer during the latter part of the flight. Thus, the skin temperature increases during the heating period, passes through a maximum, and decreases during the remainder of the flight.

Considering radiation and conduction as negligible, the heat lost by the boundary layer is equal to the heat absorbed by the skin of the model. The time rate of heat exchange between the boundary layer and the skin is

$$\frac{dQ}{dt} = h_e A_w \left(T_{aw} - T_w\right) \tag{1}$$

and the time rate of change of the heat contained in the skin is

$$\frac{dQ}{dt} = \gamma_w \tau_w A_w C_w \frac{dT_w}{dt} \tag{2}$$

Equating equations (1) and (2) and solving for the effective heat-transfer coefficient results in

$$h_e = \frac{\gamma_w C_w \tau_w \frac{dT_w}{dt}}{T_{aw} - T_w} \tag{3}$$

The properties of the wall material are known and the rate of change of wall temperature is the slope of the measured time history of the skin temperature. To obtain the temperature difference $T_{aw} - T_w$ it is first necessary to define the recovery factor.

## RECOVERY FACTOR

Recovery factor defined here has been discussed in references 5 and 6 and is briefly defined as the fraction of stagnation temperature rise, above the temperature just outside the boundary layer, attained by an insulated wall. As the stagnation temperature is constant throughout the flow, the recovery factor may be written as

$$RF = \frac{T_{aw} - T_v}{T_{s_o} - T_v} \tag{4}$$

In the absence of radiation and conduction at the peak of the skin-temperature curve, no heat is being transferred and the skin temperature and adiabatic wall temperature coincide. It is from this point that the recovery factor is determined. Trajectory and radiosonde data yield the free-stream static and stagnation temperatures. The temperature outside the boundary layer is obtained from the free-stream static temperature by correcting for the local pressure on the body.

Assuming this recovery factor to be constant during the decelerating portion of the flight, equation (4) may be re-solved to yield the time history of the adiabatic wall temperature

$$T_{aw} = T_v + RF\left(T_{s_o} - T_v\right) \tag{5}$$

This adiabatic wall temperature is the temperature that the skin would have throughout the test range if it had no heat capacity.

## ACCURACY

The error introduced in evaluating the local convective heat-transfer coefficients is caused either by inaccurate measurement of the data or by the assumptions made in the analysis. Listed in table II are the maximum values expected of these errors. As the maximums do not occur at the same time, these errors combine to give a probable maximum error in evaluating convective heat-transfer coefficients of ±6 percent for the time during which the data were used.

During the time of flight, as the skin temperature approaches its peak, the rate of change of skin temperature approaches zero, as does the temperature difference $T_{aw} - T_w$. Thus, $h_e$ becomes indeterminate. As the rate of change of skin temperature and the temperature difference $T_{aw} - T_w$ approach zero, any error in either quantity causes an increasing error in $h_e$, and the scatter in the curve of $h_e$ against time becomes large (as can be seen in fig. 9). Therefore, only the data on the smooth portion of the curve, where the probable maximum error was written ±6 percent, were used.

It can be noticed from figures 12 and 13 that the scatter between results obtained from similar stations on two different models is 3 percent, or the scatter of $\pm 1\frac{1}{2}$ percent from the mean values. It therefore appears that the actual errors are substantially less than the maximum shown by the preceding analysis.

## RESULTS AND DISCUSSION

Recovery factors shown in figure 10 were obtained for all the test stations on models A and B. Stations 8.9 on model A and 18.3 on model B had recovery factors of 0.835, while station 14.3 of model B had a recovery factor of 0.841. These were in good agreement with the recovery factor of 0.846 predicted by the theory of reference 5 $\left(RF = N_{Pr}^{1/2}\right)$ for laminar boundary layers. Recovery factors obtained for the other test stations agree with the value of 0.894 predicted by theory in reference 7 $\left(RF = N_{Pr}^{1/3}\right)$ for turbulent boundary layers. In order to evaluate these theoretical recovery factors, the thermodynamic properties of air in the Prandtl number were based on the temperature just outside the boundary layer.

Although the recovery factors obtained at three of the stations agree with the theoretical value for a laminar boundary layer, only station 8.9 on model A has a Reynolds number range that is likely to accompany a laminar boundary layer. All the heat-transfer coefficients were of the same order of magnitude and were of a magnitude expected for a turbulent boundary layer. This suggests that these three stations were in a transition region where it may have been possible to obtain laminar recovery factors in conjunction with turbulent heat transfer. This view is supported by Eber's tests on cones, at Mach numbers from 1.2 to 3.1 (ref. 8), in which the heat-transfer data indicated that transition occurred on the cones, but the measured recovery factors along the cones were equal to the values predicted by the theory for laminar flow.

Time histories of the measured skin temperatures and the calculated adiabatic wall temperatures are shown in figure 11 for stations 8.9 and 123.5 of model A. The skin-temperature curves show the variation in the magnitude and time of occurrence of the maximum skin temperature measured at the extreme test stations on the body; that is, a maximum skin temperature of 398° F at 5.35 seconds for station 8.9 and a maximum skin temperature of 279° F at 7.94 seconds for station 123.5. The greater rate of heat transfer and thinner skin at the forward station cause the skin temperature there to rise faster and reach a higher peak than at the aft station, even though the adiabatic wall temperature at the forward station is less than that at the aft station. During the cooling part of the flight, when the adiabatic wall temperature is lower than the skin temperature at a given station, the greater rate of heat transfer and thinner skin at station 8.9 result in a higher rate of skin cooling at station 8.9 than at station 123.5.

The heat-transfer data obtained in the present test are presented in figure 12 in terms of Nusselt, Prandtl, and Reynolds numbers. The temperature used to evaluate the viscosity, conductivity, density, velocity, and specific heat of the air in the aforementioned parameters is the temperature just outside the boundary layer $T_v$. The flow conditions just outside the boundary layer were determined by correcting the free-stream conditions for the theoretical pressure distribution, which was obtained from reference 9. (Although theoretical, the pressure distributions thus obtained have been substantiated by the wind-tunnel test of ref. 10.)

As can be seen from figure 12, the heat-transfer parameter $N_{Nu}N_{Pr}^{-1/3}$ is primarily a function of Reynolds number rather than body station; that is, results obtained at different body stations were the same when the Reynolds numbers were equal. Although it is expected that the body contour would have some effect on the heat transfer, there was no apparent effect on the high-fineness-ratio body used for this investigation.

It would be more convenient in reducing the heat-transfer data for engineering purposes to base the heat-transfer parameters, Nusselt,

Prandtl, and Reynolds numbers, on conditions of the air in the undisturbed free stream ahead of the model. The results thus obtained are shown in figure 13. This correlation is in good agreement with the correlation based on local conditions, probably because the free-stream conditions are not very different from local conditions for this high-fineness-ratio body.

The equation for thermal conductance for turbulent flow over a flat plate at subsonic speeds is given as $N_{Nu} = 0.0296\ R^{0.8} N_{Pr}^{1/3}$ in reference 11. This equation results from frictional drag measurements on a flat plate in parallel turbulent flow as correlated by Colburn (ref. 12) using a momentum heat-transfer analogy. The dashed line shown in figures 12 and 13 represents the preceding equation. This line falls remarkably close to the test data obtained on the parabolic body of revolution at supersonic speeds and is in agreement with the test results correlated either on flow conditions just outside the boundary layer or on free-stream conditions. While the agreement is better at the higher Reynolds number, this equation could be used to evaluate the heat-transfer coefficient with fair accuracy over the entire range of Reynolds numbers shown.

Investigations similar to those described in this paper were conducted on two V-2 research missiles. Figure 4 of reference 13 shows the results from the heat-transfer tests on the V-2 research missiles compared with Eber's correlation (ref. 8), that is, as a plot of Nusselt number against Reynolds number. For convenience, the letter designations for the stations are identified with those used in reference 13. These stations in inches from the nose are as follows:

| Configuration | Station | Distance from nose, in. |
|---|---|---|
| V-2 No. 27 | A | 2.5 |
| | C | 6.0 |
| | G | 12.0 |
| | H | 12.0 (trip) |
| | K | 84.4 |
| | M | 121.4 |
| V-2 No. 19 | --- | 41.71 |

The thermal conductivity and viscosity of the air were based on the adiabatic wall temperature and the density and velocity on conditions just outside the boundary layer. These results are reproduced in figure 14. The line faired through the points is 40 percent above the

Eber line. For further comparison the RM-10 heat-transfer data, based on the same flow properties, are also shown. A line faired through the RM-10 test results is approximately 60 percent above Eber or 20 percent above the V-2 line.

Results from the V-2 tests shown in figure 14 are expressed in figure 15 as $N_{Nu}N_{Pr}^{-1/3}$ plotted against Reynolds number based on conditions of the air just outside the boundary layer. Reference 13 states that the decrease at lower Reynolds number in the points M and K for the V-2 No. 27 and for the point of V-2 No. 19 is attributed to partial transition. Neglecting these points at the low Reynolds number, the V-2 heat-transfer data are approximately 15 percent lower than the RM-10 data represented by the solid curve. The correlation $N_{Nu}N_{Pr}^{-1/3} = 0.0296\ R^{0.8}$ is shown as a dashed line and falls approximately 20 percent higher than the V-2 points.

In figure 16, the heat-transfer parameters $N_{Nu}N_{Pr}^{-1/3}$ from the RM-10 data are plotted against Reynolds number. The thermal conductivity, viscosity, and specific heat of air are based on adiabatic wall temperature, and the density is based on conditions just outside the boundary layer. For this temperature basis, somewhat greater scatter can be seen in the test points. The faired line through the test points falls approximately 20 percent lower than the flat-plate correlation $N_{Nu}N_{Pr}^{-1/3} = 0.0296\ R^{0.8}$.

The V-2 data are expressed to the same basis as in figure 16 and are shown in figure 17. For comparison, the RM-10 faired curve and the flat-plate correlation $N_{Nu}N_{Pr}^{-1/3} = 0.0296\ R^{0.8}$ are also shown in this figure. The V-2 points fall about 15 percent lower than the RM-10 faired curve and approximately 35 percent lower than the flat-plate equation.

Heat-transfer parameters $N_{Nu}N_{Pr}^{-1/3}$ for the RM-10 data are plotted (fig. 18) against Reynolds number. The thermal conductivity, viscosity, and density of the air are based on the wall temperature. The solid line in the figure is the faired curve of the RM-10 points. Reference 14 gives a theory for heat transfer on cones in a supersonic turbulent boundary layer $\left(N_{Nu}N_{Pr}^{-1/3} = 0.034\ R^{0.8}\right)$ that is approximately 7 percent lower than the curved line representing the RM-10 points. The flat-plate equation $N_{Nu}N_{Pr}^{-1/3} = 0.0296\ R^{0.8}$ is shown in the figure as a dashed line and is approximately 20 percent lower than the RM-10 faired curve.

In figure 19, the V-2 heat-transfer parameters are plotted against Reynolds number. The thermal conductivity, viscosity, and density are based on wall temperature. Disregarding again for low Reynolds number the points K and M and V-2 No. 19 shows the V-2 heat-transfer data to be roughly 15 percent lower than the RM-10 faired curve reproduced from figure 18. A line representing the cone theory $\left(N_{Nu}N_{Pr}^{-1/3} = 0.034\ R^{0.8}\right)$ falls approximately 8 percent above the V-2 data. The flat-plate correlation $N_{Nu}N_{Pr}^{-1/3} = 0.0296\ R^{0.8}$ is shown by a dashed line approximately 6 percent lower than the V-2 points.

The agreement between the same approximate stations on models A and B is well within the estimated accuracy. From the various methods of correlation it appears that by basing the properties of the air on the temperature just outside the boundary layer and on wall temperature gave results that were approximately 15 percent above the V-2 heat-transfer data and also were in good agreement with the referenced equations.

## CONCLUSIONS

Supersonic convective heat transfer has been measured in flight on two models of the NACA RM-10 missile. The Mach numbers covered by the tests were from 1.02 to 2.48 and the Reynolds numbers were from $3.18 \times 10^6$ to $163.85 \times 10^6$ based on the axial distance from the nose to the stations where the skin-temperature measurements were made.

Results of the tests indicate that:

1. Heat-transfer parameters from the RM-10 data when correlated on a Nusselt, Prandtl, and Reynolds number relation, based on conditions just outside the boundary layer, showed that the equation for convective heat transfer on a flat plate in a subsonic flow $\left(N_{Nu}N_{Pr}^{-1/3} = 0.0296\ R^{0.8}\right)$ was in good agreement with the test results, and the results from the V-2 tests were approximately 15 percent lower than the RM-10 data.

2. Correlation of the heat-transfer parameters for the RM-10 on wall temperature showed that the equation for cones for convective heat transfer in a supersonic turbulent boundary layer $\left(N_{Nu}N_{Pr}^{-1/3} = 0.034\ R^{0.8}\right)$ was in good agreement with the test results and the results from the V-2 tests were approximately 15 percent lower than the RM-10 data.

3. The RM-10 heat-transfer data are approximately 60 percent higher than Eber's empirical equation.

4. Good agreement was obtained between the heat-transfer coefficients of models A and B and the scatter is within the estimated accuracy of ±6 percent.

5. Recovery factors measured along the body are in agreement with the flat-plate theory.

6. No evidence of boundary-layer transition was apparent in the heat-transfer data.

Langley Aeronautical Laboratory,
National Advisory Committee for Aeronautics,
Langley Field, Va., January 18, 1951.

## REFERENCES

1. Fricke, Clifford L., and Smith, Francis B.: Skin-Temperature Telemeter for Determining Boundary-Layer Heat-Transfer Coefficients. NACA RM L50J17, 1951.

2. Morrow, John D., and Katz, Ellis: Flight Investigation at Mach Numbers From 0.6 to 1.7 To Determine Drag and Base Pressures on a Blunt-Trailing-Edge Airfoil and Drag of Diamond and Circular-Arc Airfoils at Zero Lift. NACA TN 3548, 1955. (Supersedes NACA RM L50E19a.)

3. Keenan, Joseph H., and Kaye, Joseph: Thermodynamic Properties of Air Including Polytropic Functions. John Wiley & Sons, Inc., 1945.

4. Kelly, K. K.: Contributions to the Data on Theoretical Metallurgy. II. High-Temperature Specific-Heat Equations for Inorganic Substances. Bulletin 371, Bur. Mines, 1934, p. 32.

5. Wimbrow, William R.: Experimental Investigation of Temperature Recovery Factors on Bodies of Revolution at Supersonic Speeds. NACA TN 1975, 1949.

6. Stalder, Jackson R., Rubesin, Morris W., and Tendeland, Thorval: A Determination of the Laminar-, Transitional-, and Turbulent-Boundary-Layer Temperature-Recovery Factors on a Flat Plate in Supersonic Flow. NACA TN 2077, 1950.

7. Squire, H. B.: Heat Transfer Calculation for Aerofoils. R. & M. No. 1986, British A.R.C., 1946.

8. Eber, [G.]: Experimental Research on Friction Temperature and Heat Transfer for Simple Bodies at Supersonic Velocities. Rep. GTR 22, Chance Vought Aircraft Translation, May 20, 1946.

9. Jones, Robert T., and Margolis, Kenneth: Flow Over a Slender Body of Revolution at Supersonic Velocities. NACA TN 1081, 1946.

10. Esenwein, Fred T., Obery, Leonard J., and Schueller, Carl F.: Aerodynamic Characteristics of NACA RM-10 Missile in 8- by 6-Foot Supersonic Wind Tunnel at Mach Numbers From 1.49 to 1.98. II - Presentation and Analysis of Force Measurements. NACA RM E50D28, 1950.

11. Johnson, H. A., Rubesin, M. W., et al.: A Design Manual for Determining the Thermal Characteristics of High Speed Aircraft (Reprint). AAF TR No. 5632, Air Materiel Command, U. S. Air Force, Sept. 10, 1947.

12. Colburn, Allan P.: A Method of Correlating Forced Convection Heat Transfer Data and a Comparison With Fluid Friction. Trans. Am. Inst. Chem. Eng., vol. XXIX, 1933, pp. 174-210.

13. Fischer, W. W.: Supersonic Convective Heat Transfer Correlations From Skin-Temperature Measurements During Flights of V-2 Rockets No. 27 and No. 19. Rep. No. 55258, Gen. Elec. Co., July 1949.

14. Gazley, C., Jr.: Theoretical Evaluation of the Turbulent Skin-Friction and Heat Transfer on a Cone in Supersonic Flight. Rep. No. R49A0524, Gen. Elec. Co., Nov. 1949.

TABLE I.- SKIN THICKNESS AT TEST STATIONS

| Model | Station (1) | Skin thickness, in. |
|---|---|---|
| A | 8.9 | 0.0587 |
| | 17.8 | .0587 |
| | 36.2 | .0927 |
| | 49.9 | .0816 |
| | 86.1 | .0933 |
| | 123.5 | .0863 |
| B | 14.3 | 0.0591 |
| | 18.3 | .0591 |
| | 85.3 | .0935 |

[1]Station number denotes axial distance from nose measured in inches.

TABLE II.- ACCURACY

| Sources of error | Maximum error in convective heat-transfer coefficient, percent |
|---|---|
| A possible error in measured skin temperatures of ±2 percent of maximum skin temperature at that station | ±4 |
| Summation of temperature lag through the skin and of the thermometer | ±1 |
| Possible ±2 percent error in skin thickness | ±2 |
| Neglected heat flows in making heat balances | $\pm 4\frac{1}{2}$ |

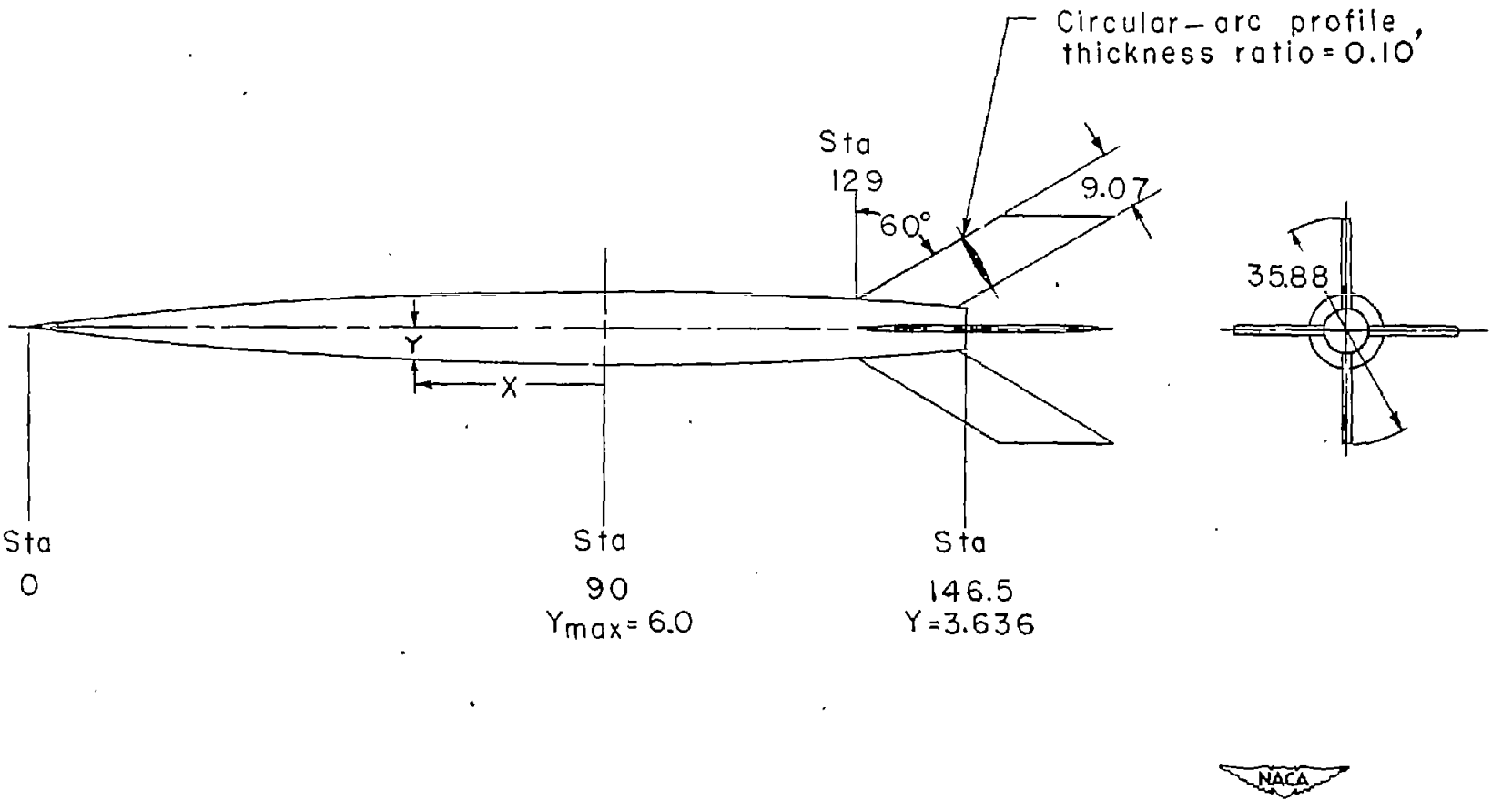


Figure 1.- General configuration and body equation of the NACA RM-10. Dimensions are in inches. Station number denotes axial distance from nose in inches. Body profile equation $Y = 6.000 - 0.0007407X^2$

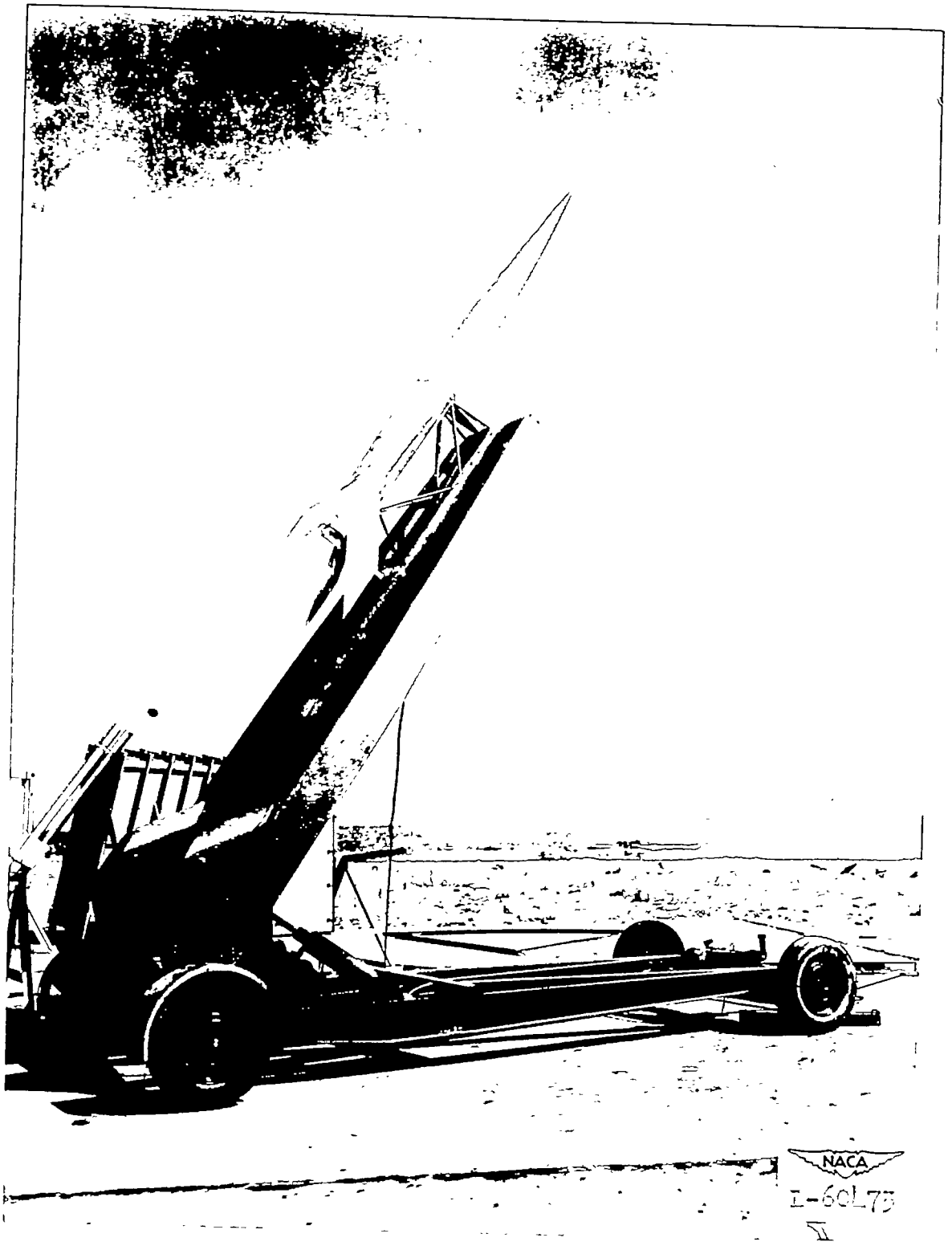


Figure 2. Photograph of model in launching position.

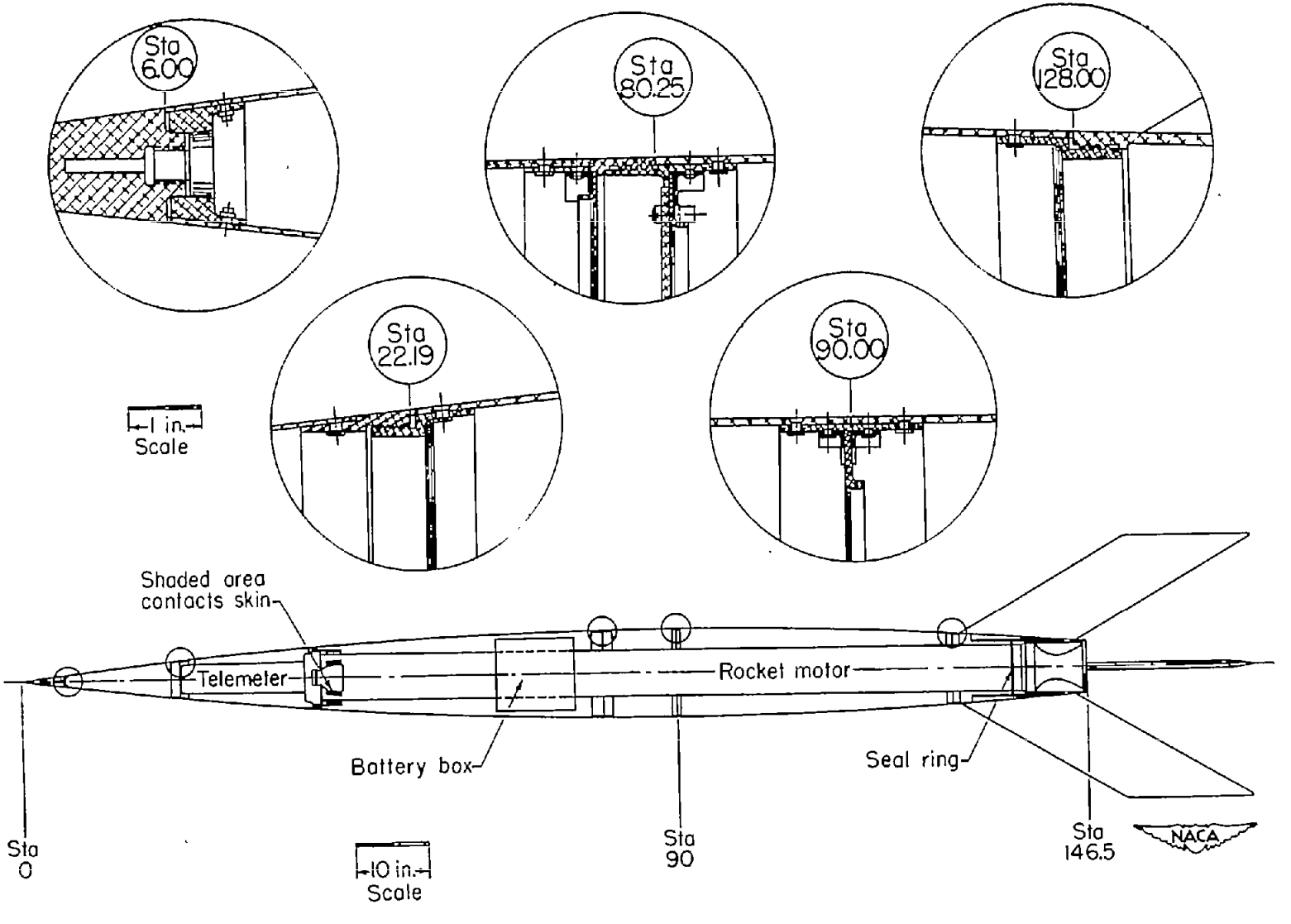


Figure 3.- Internal construction of the NACA RM-10.

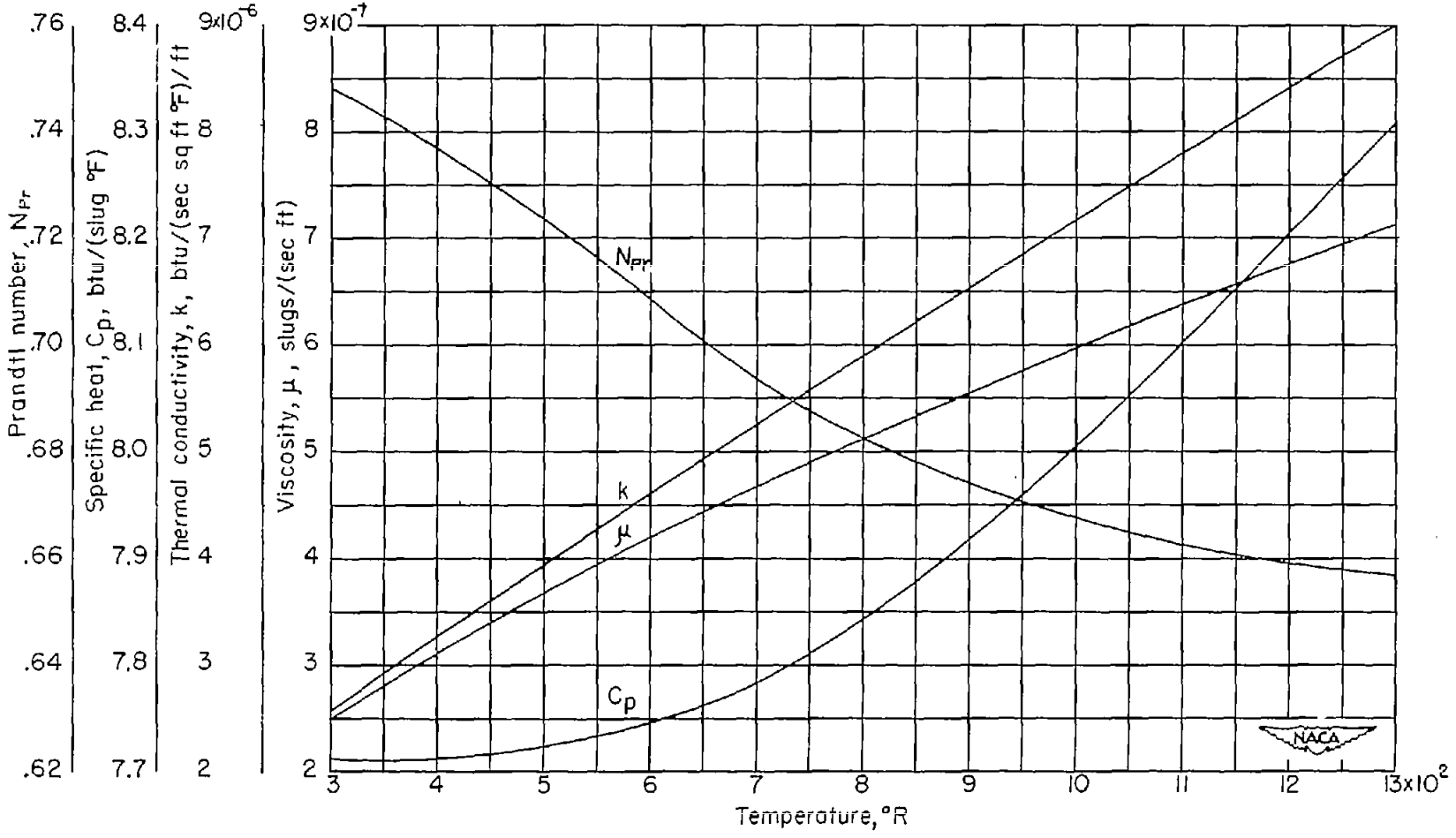


Figure 4.- Thermodynamic properties of air.

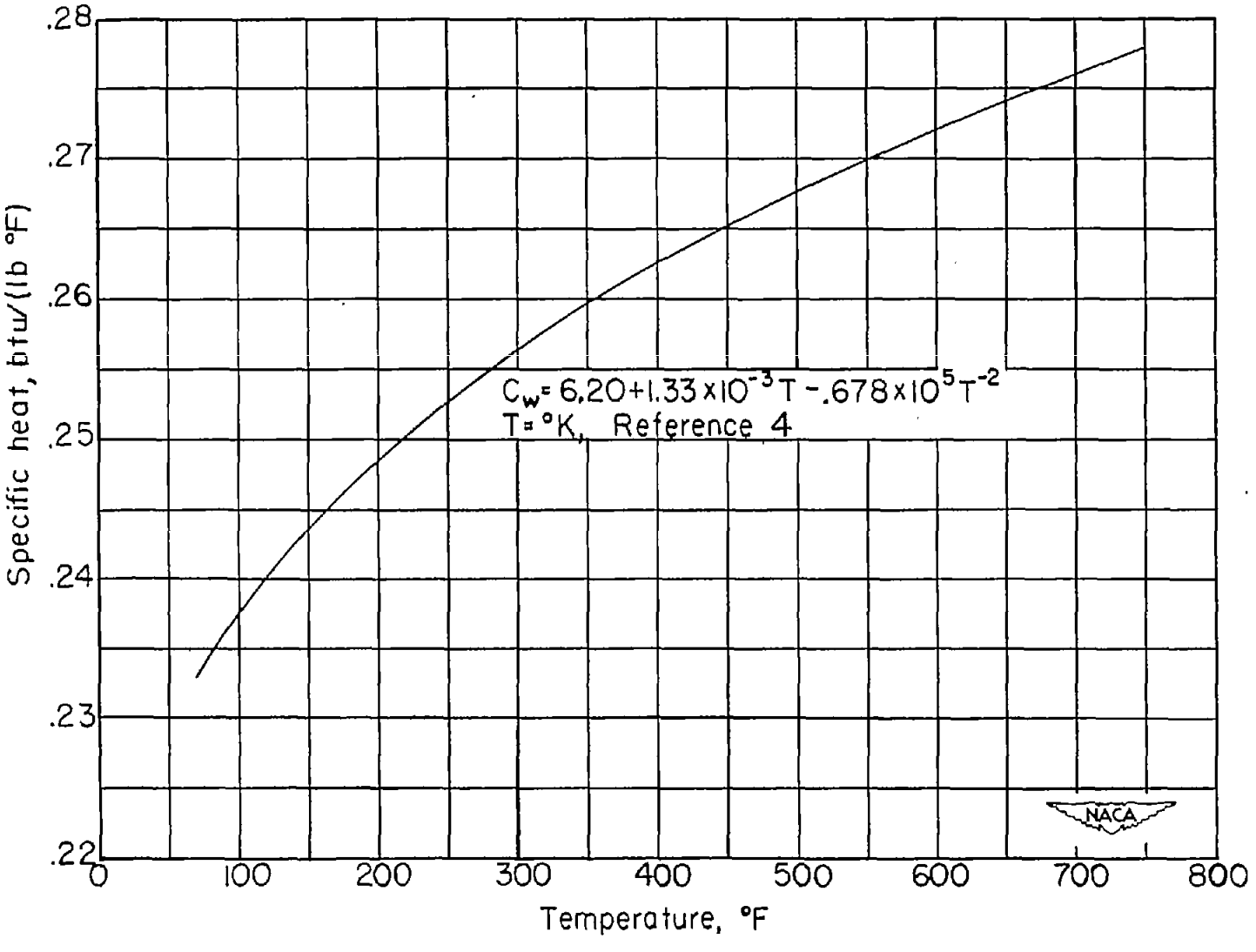


Figure 5.- Specific heat of magnesium.

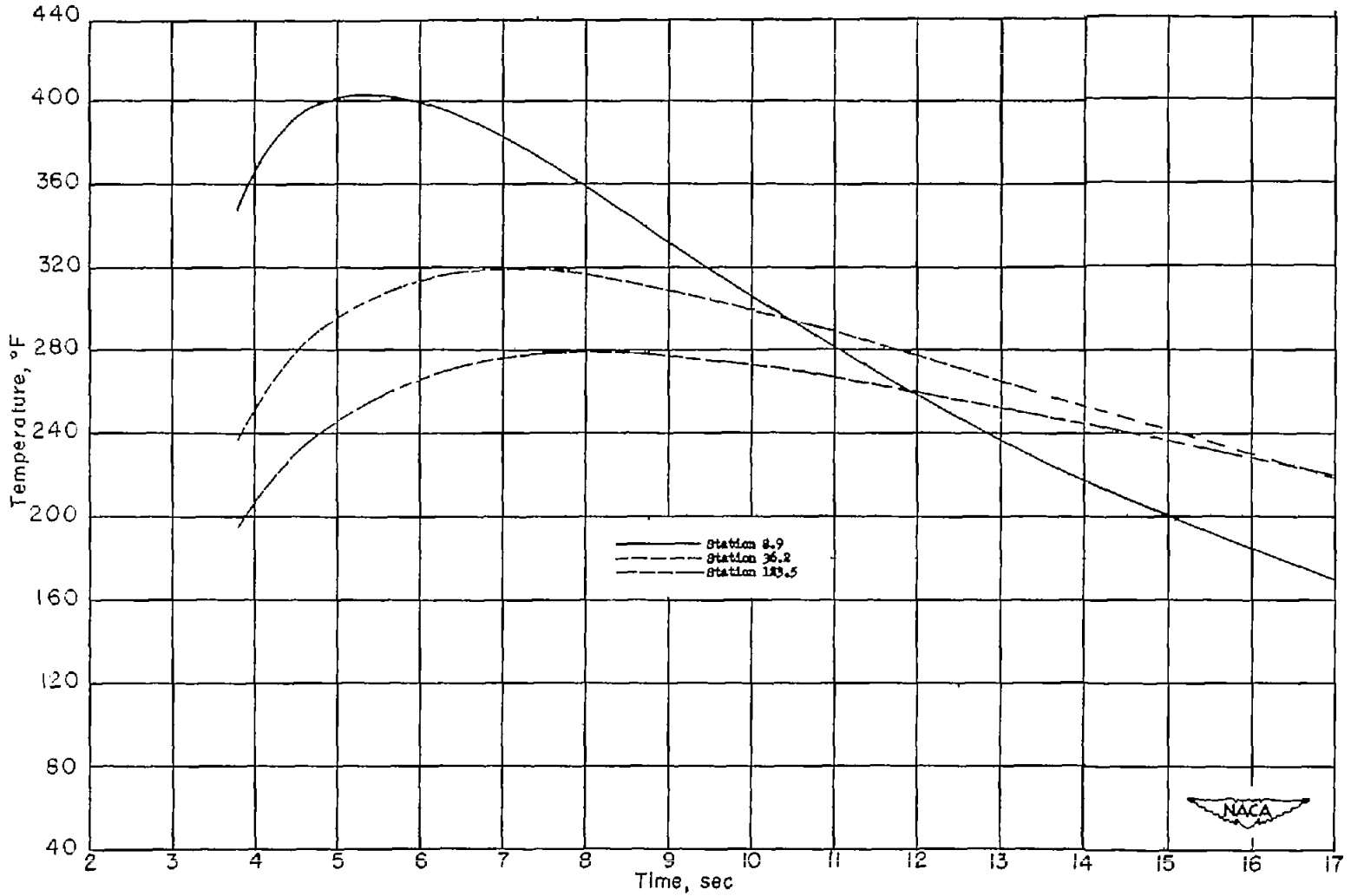


(a) Model A.

Figure 6.- Skin-temperature time history.

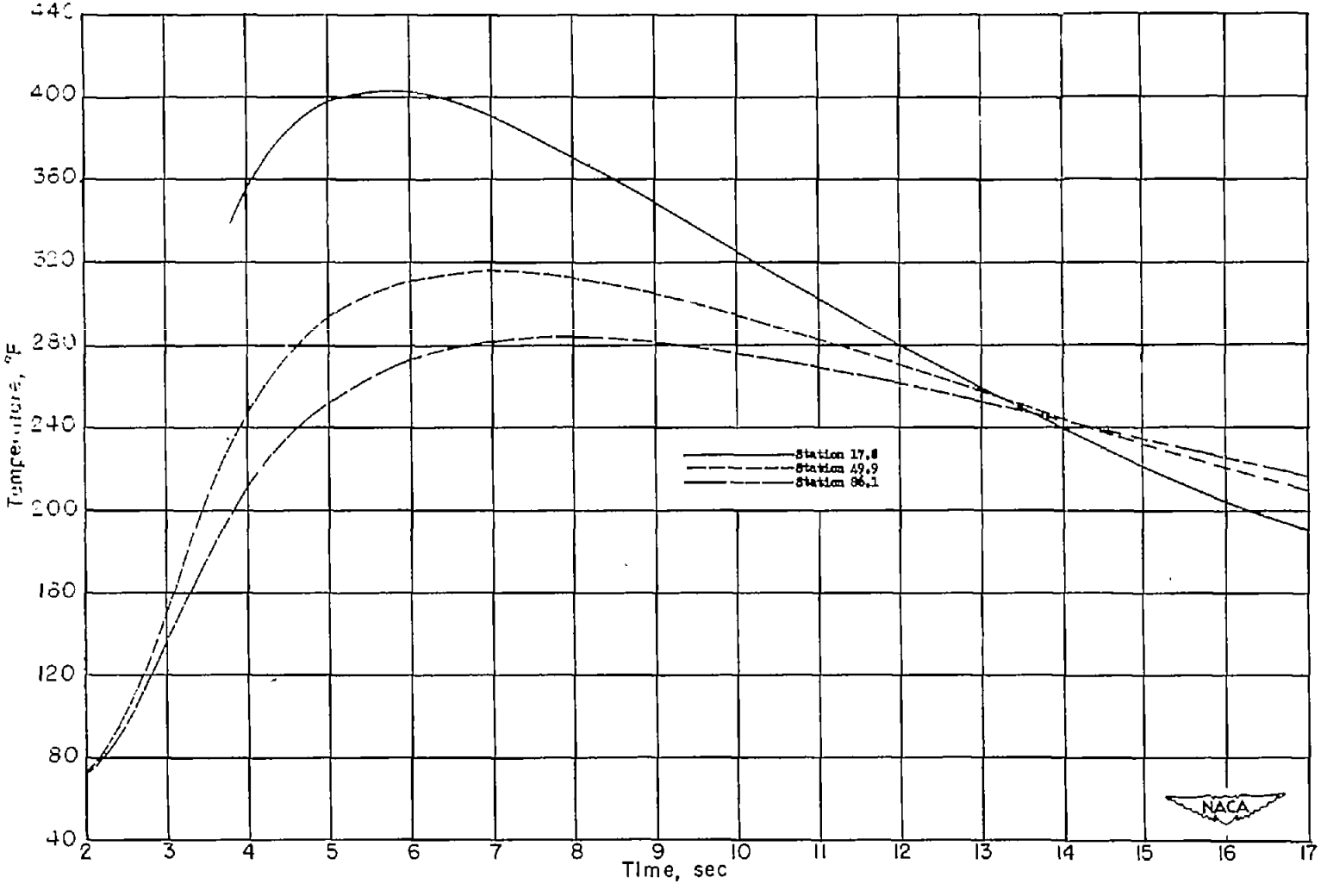


(a) Concluded.

Figure 6.- Continued.

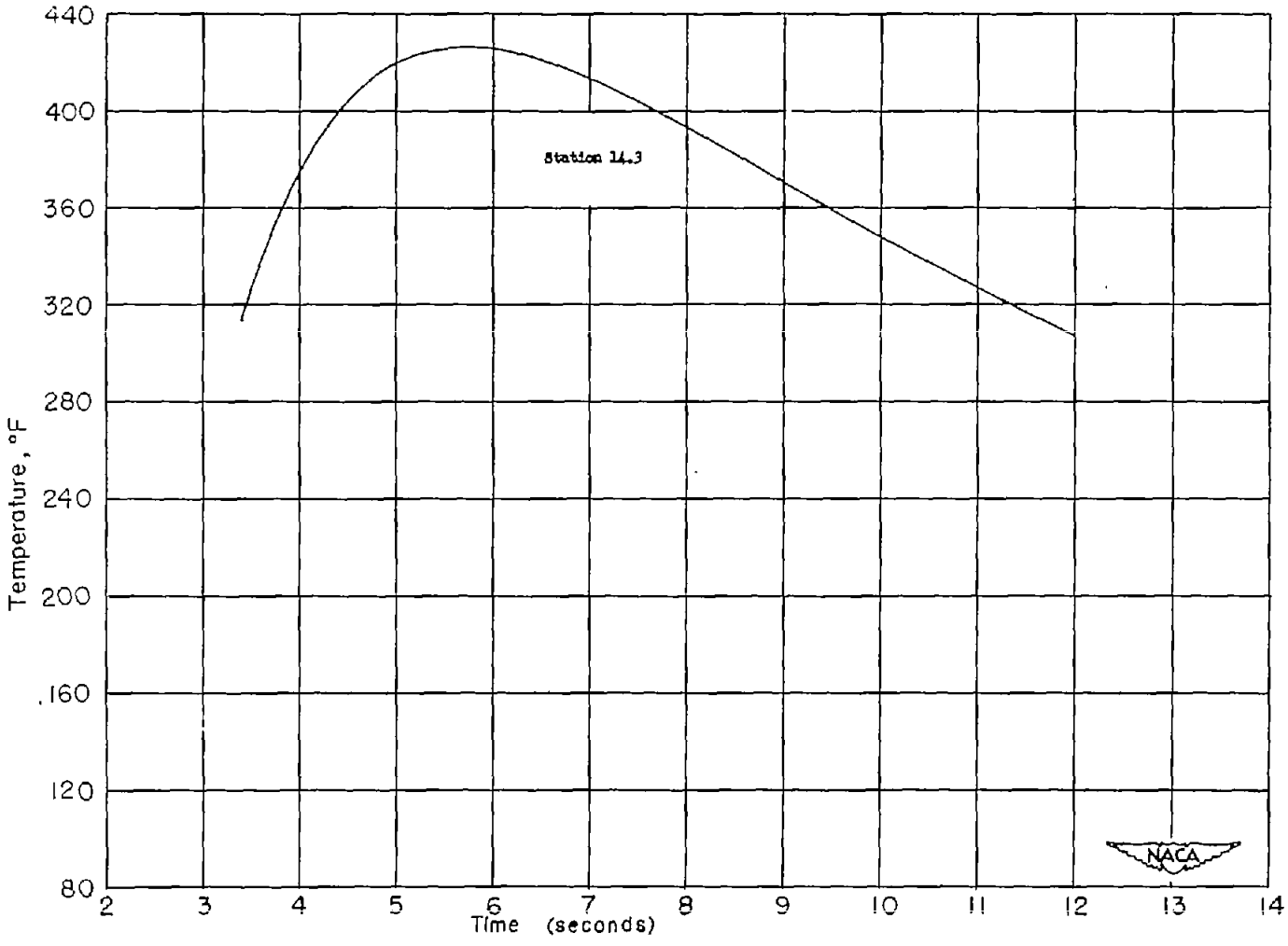


(b) Model B.

Figure 6.- Continued.

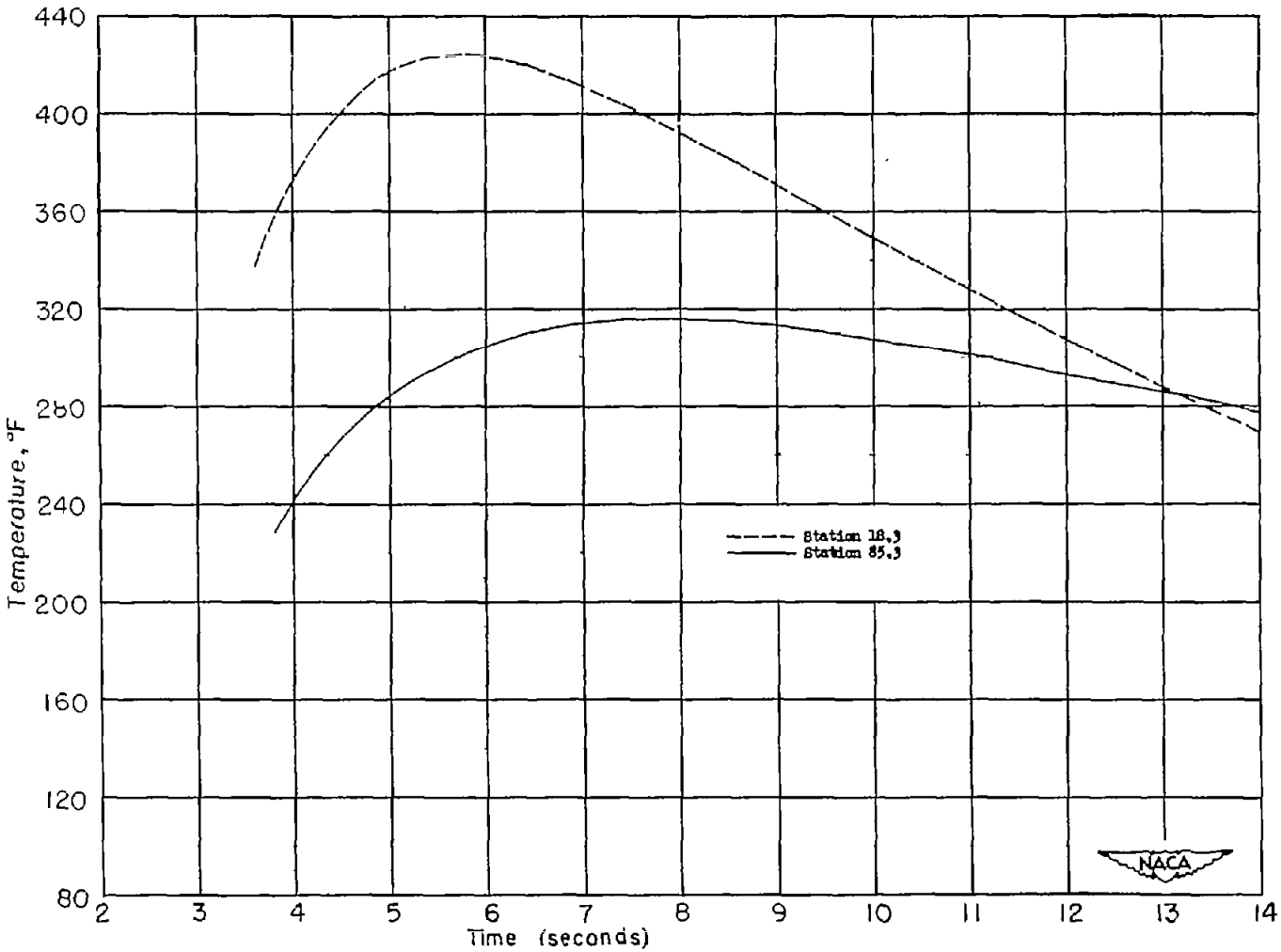


(b) Concluded.

Figure 6.- Concluded.

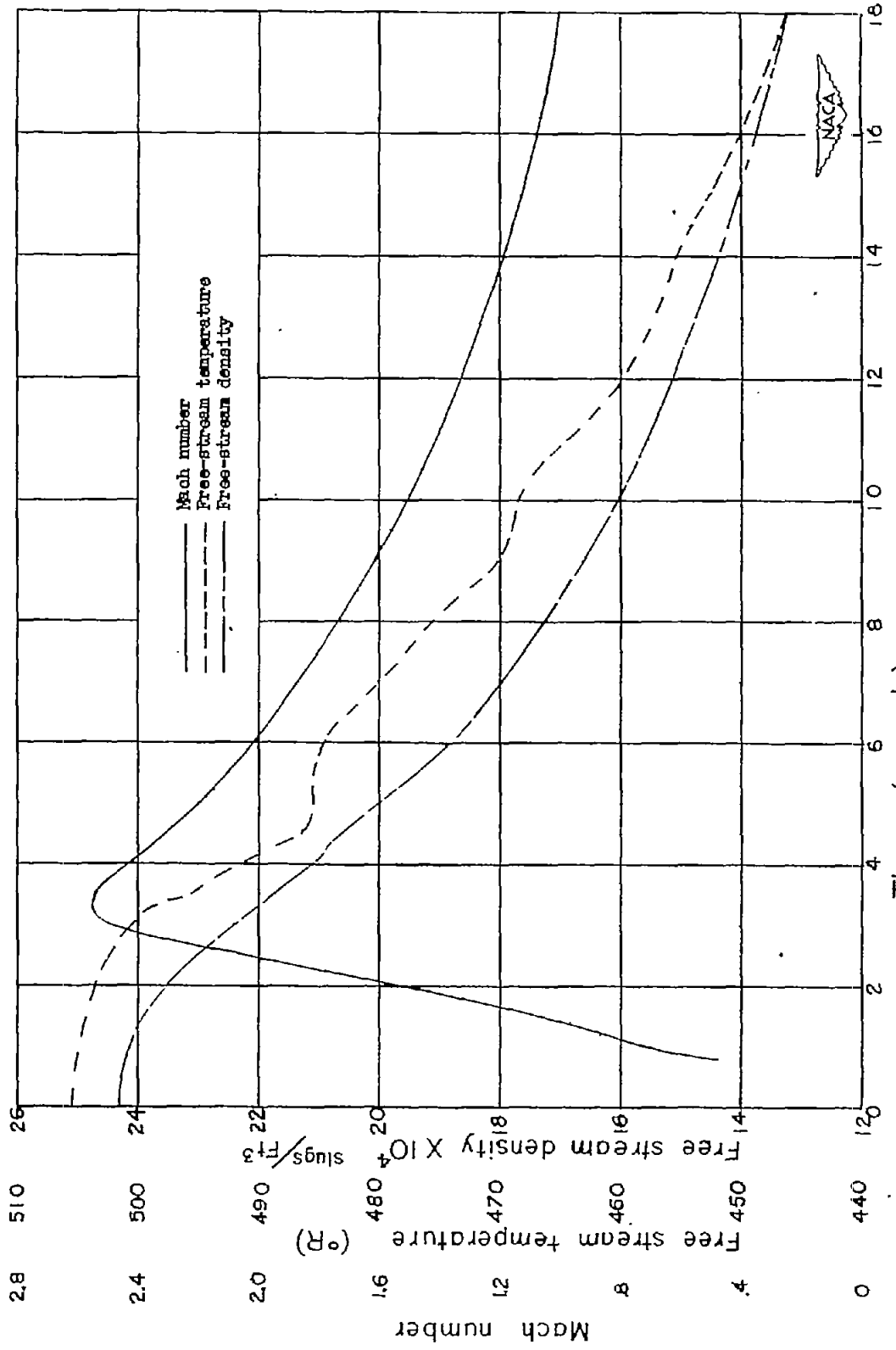


(a) Model A.

Figure 7.- Free-stream parameters.

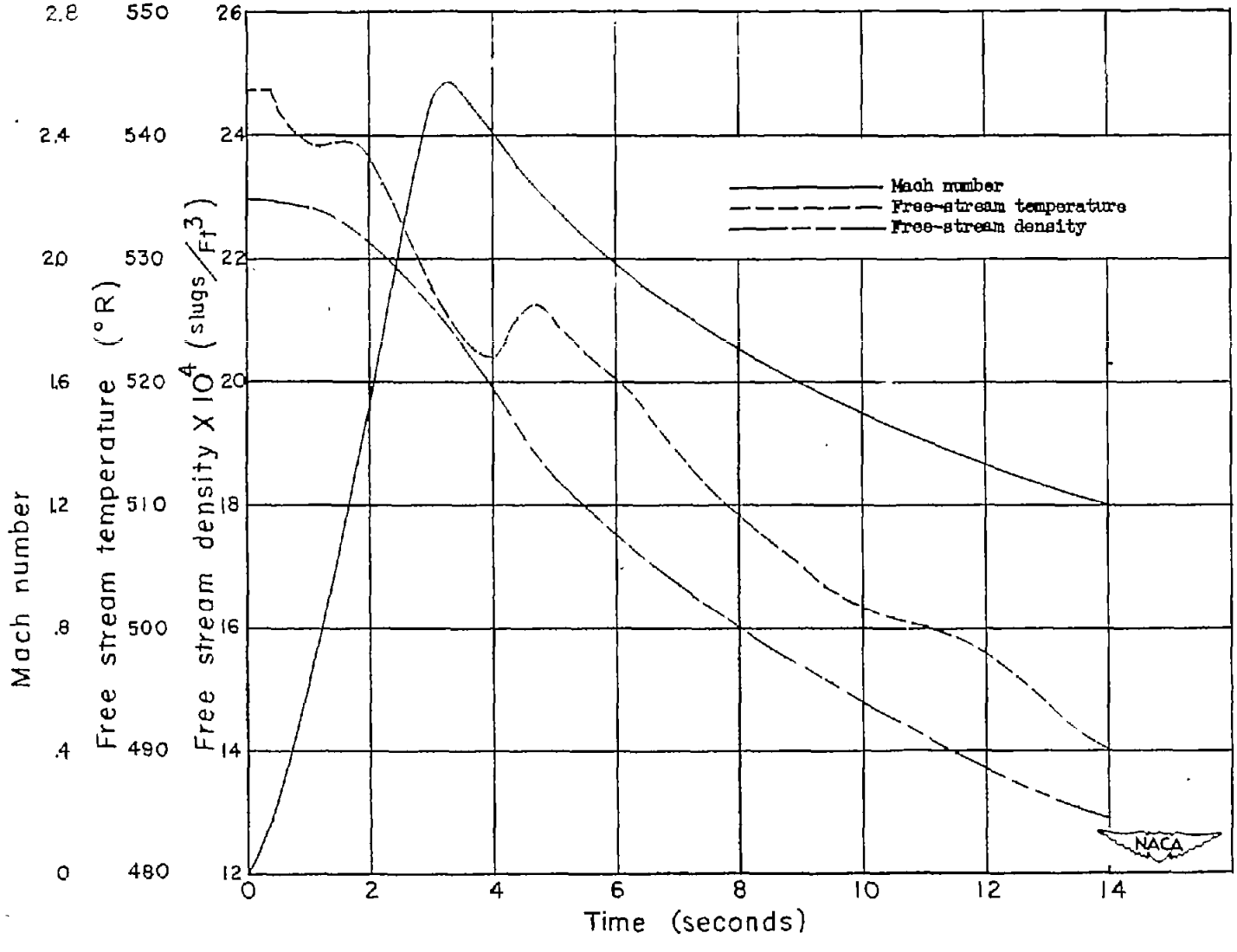


(b) Model B.

Figure 7.- Concluded.

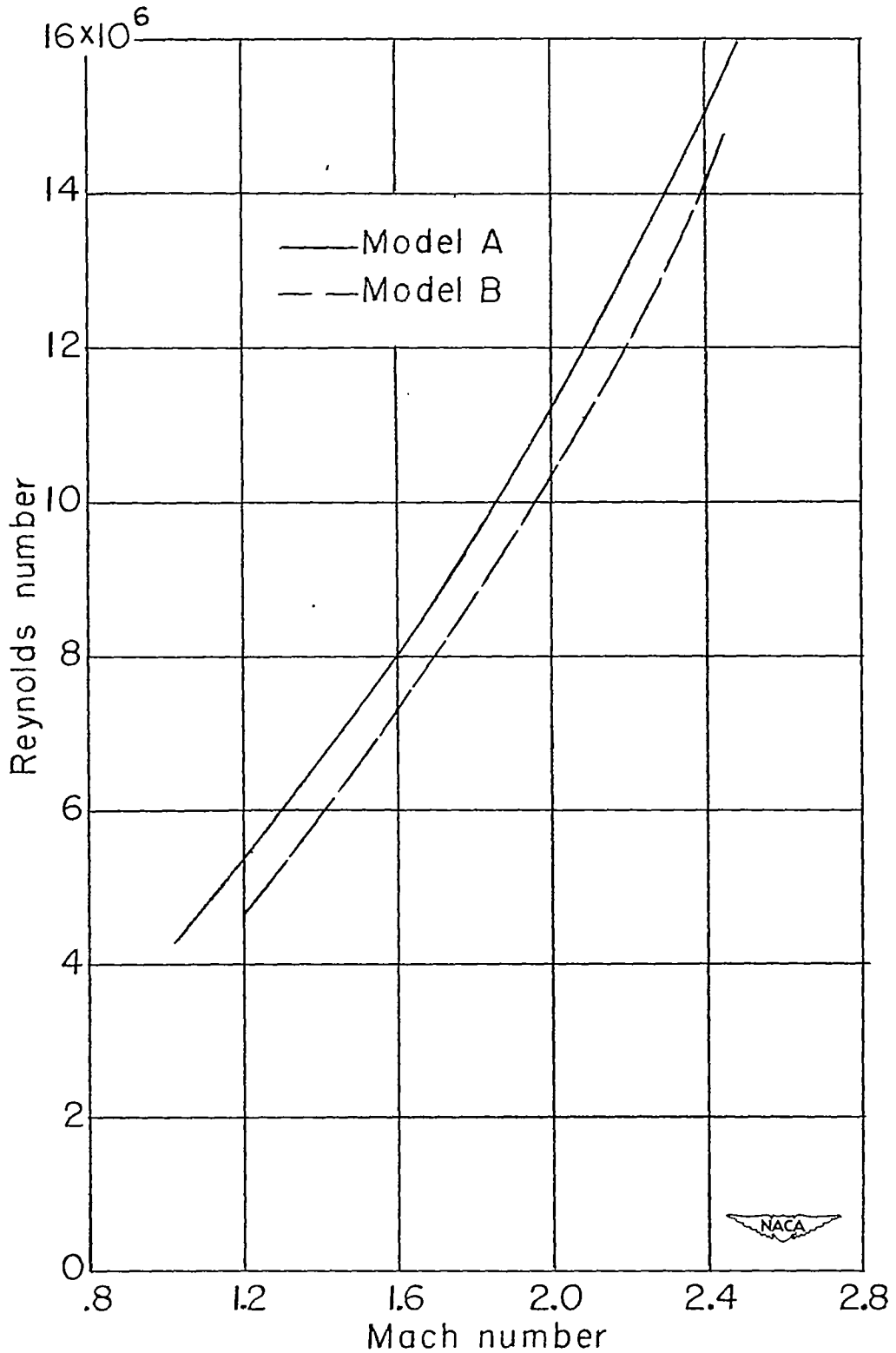


Figure 8.- Reynolds number per foot (based on the condition of the air in the undisturbed free stream ahead of the model).

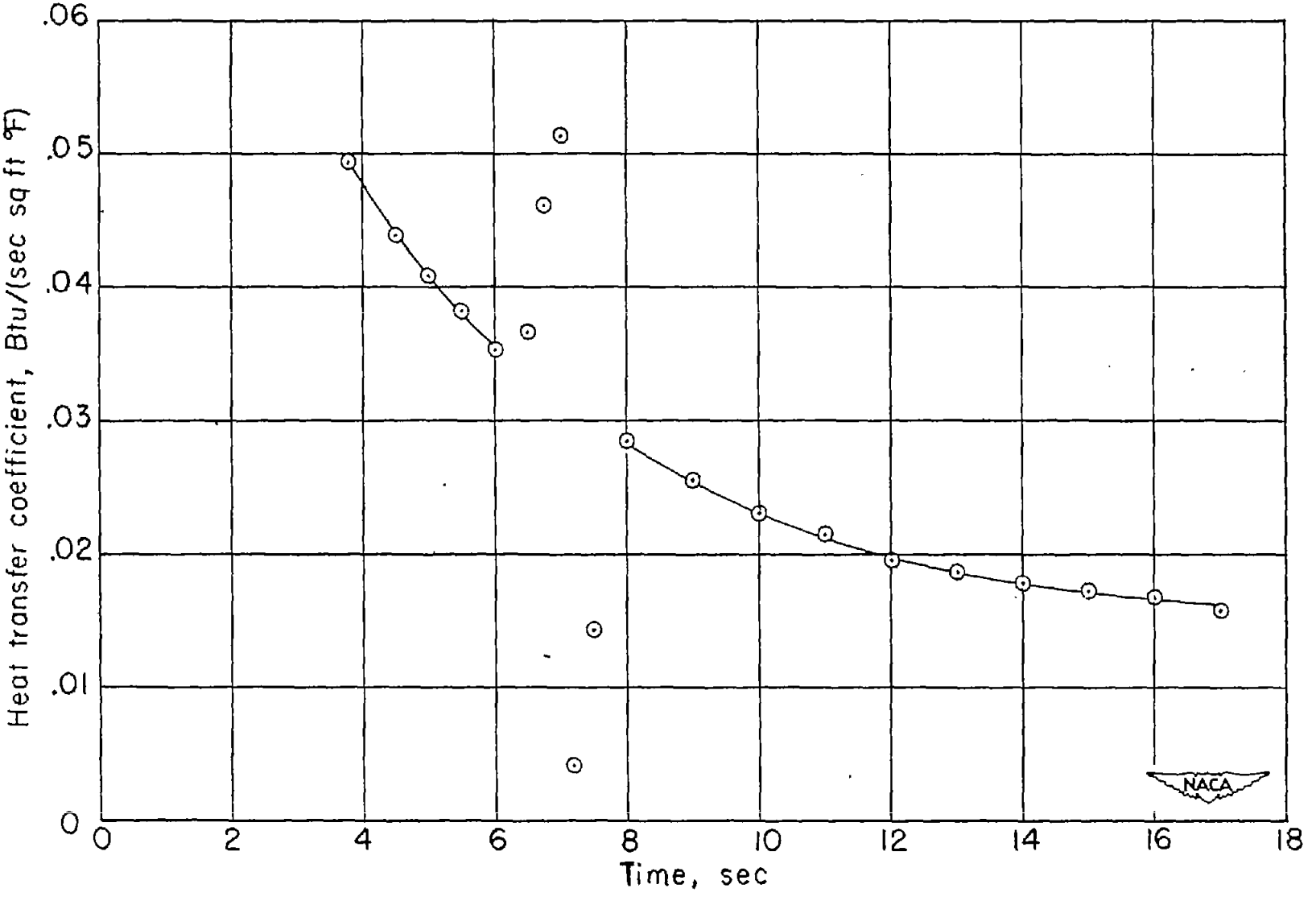


Figure 9.- Typical variation of heat-transfer coefficient with time.

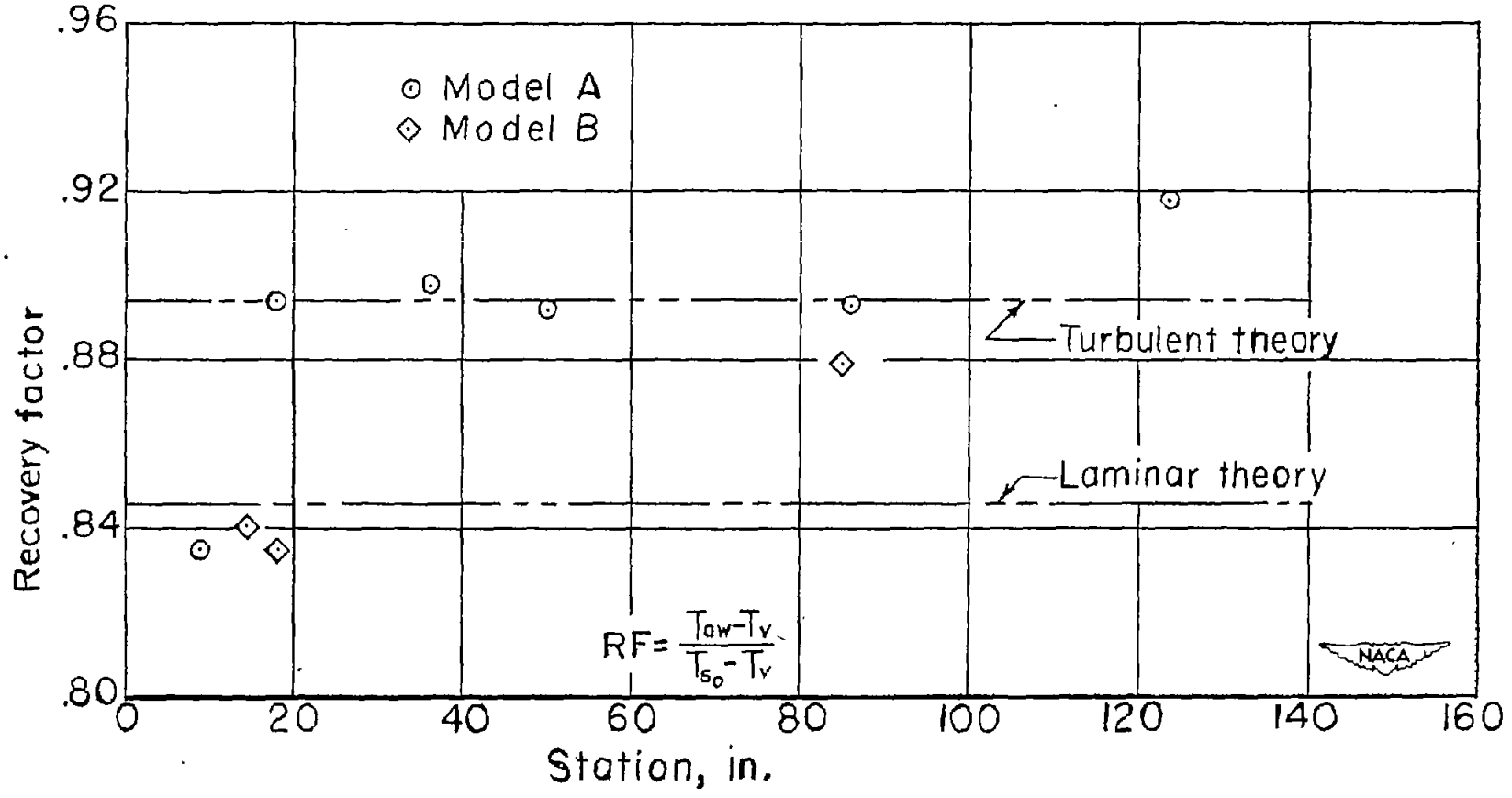


Figure 10.- Recovery factors obtained at the test stations on the vehicle.

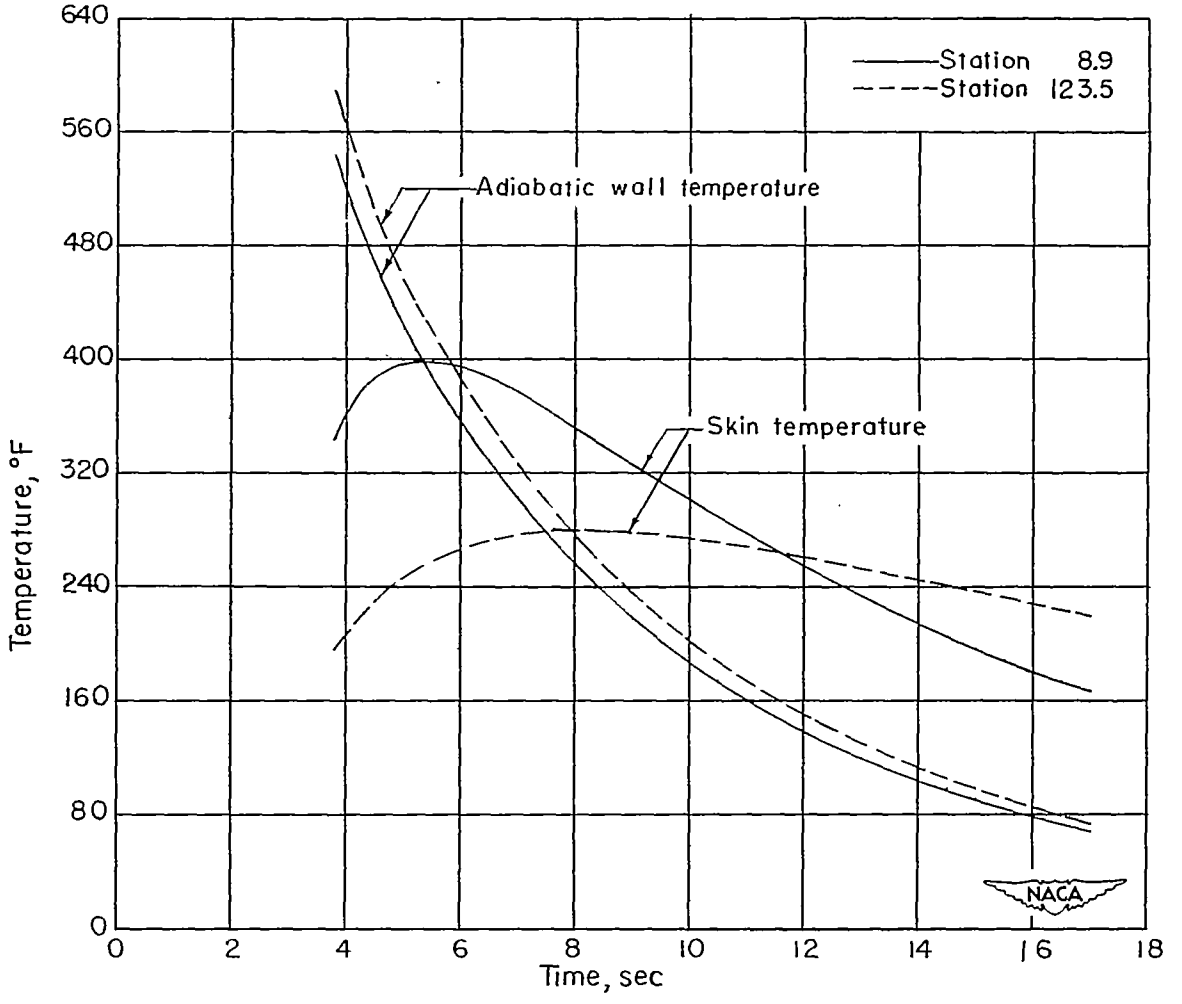


Figure 11.- Typical time histories of skin temperature and adiabatic wall temperature.

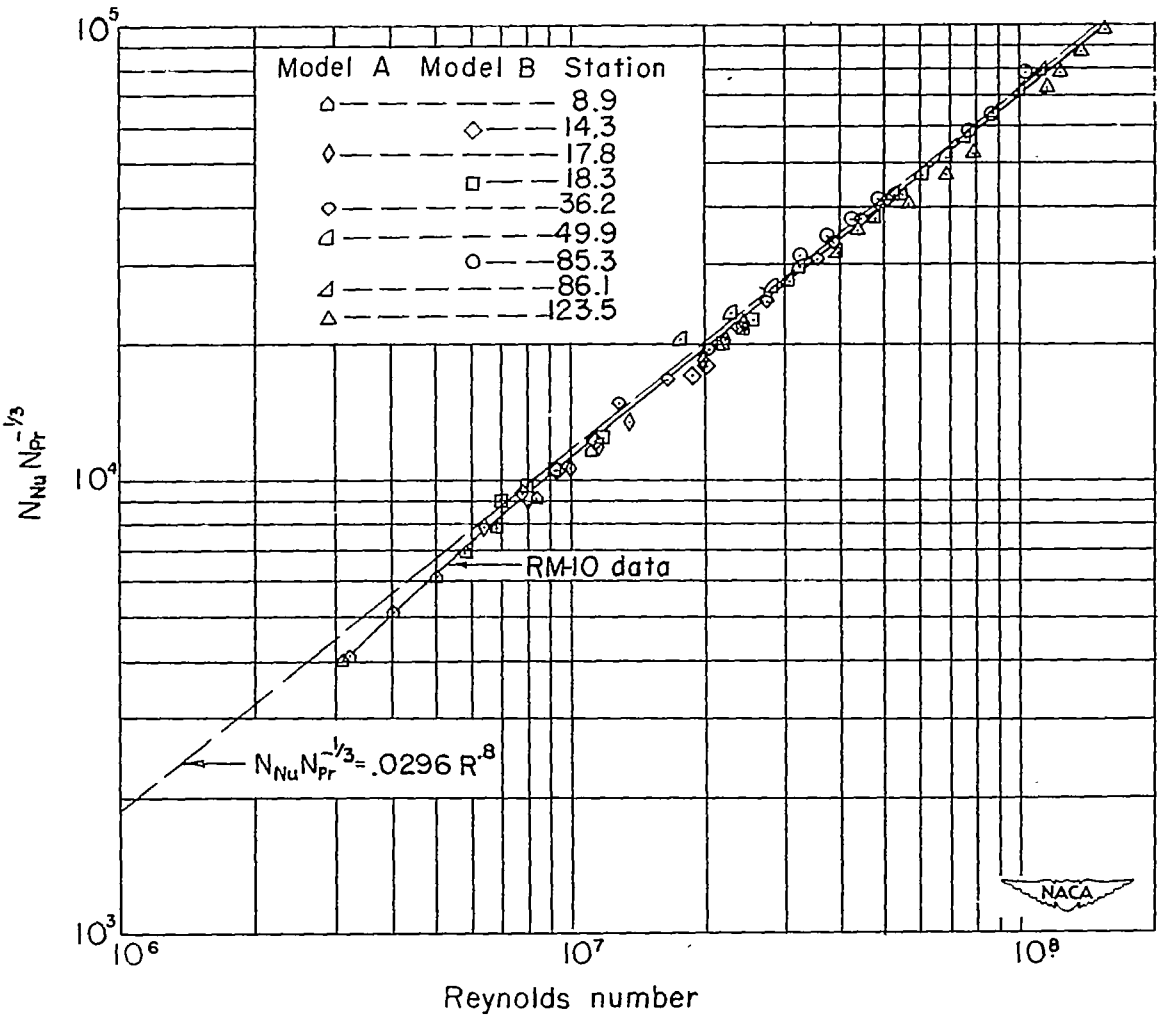


Figure 12.- Correlation of heat-transfer data (based on temperature outside the boundary layer) with Colburn's turbulent flat-plate formula (ref. 12).

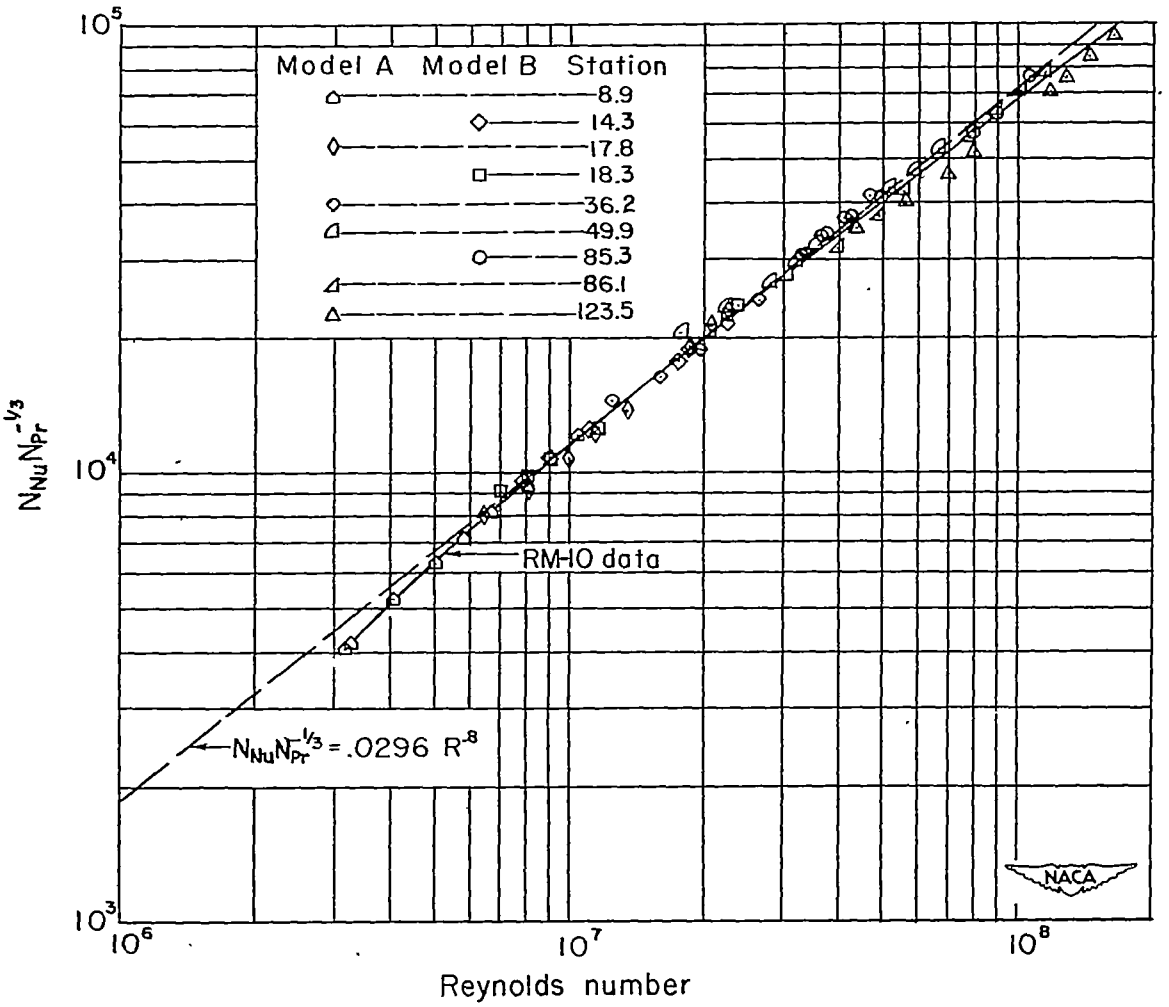


Figure 13.- Correlation of heat-transfer data (based on free-stream temperature) with Colburn's turbulent flat-plate formula.

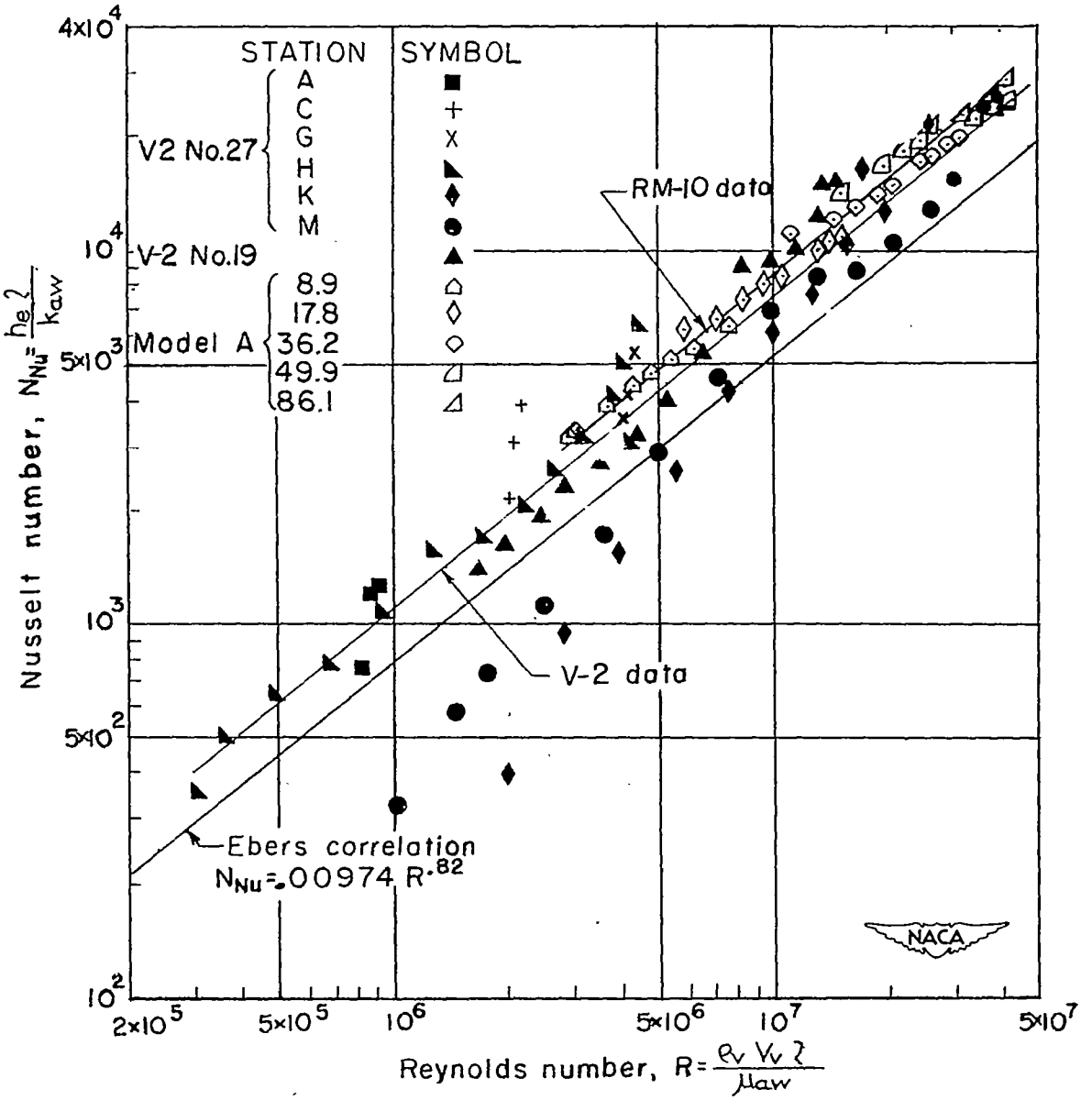


Figure 14.- Correlation of V-2 heat-transfer data with Eber.

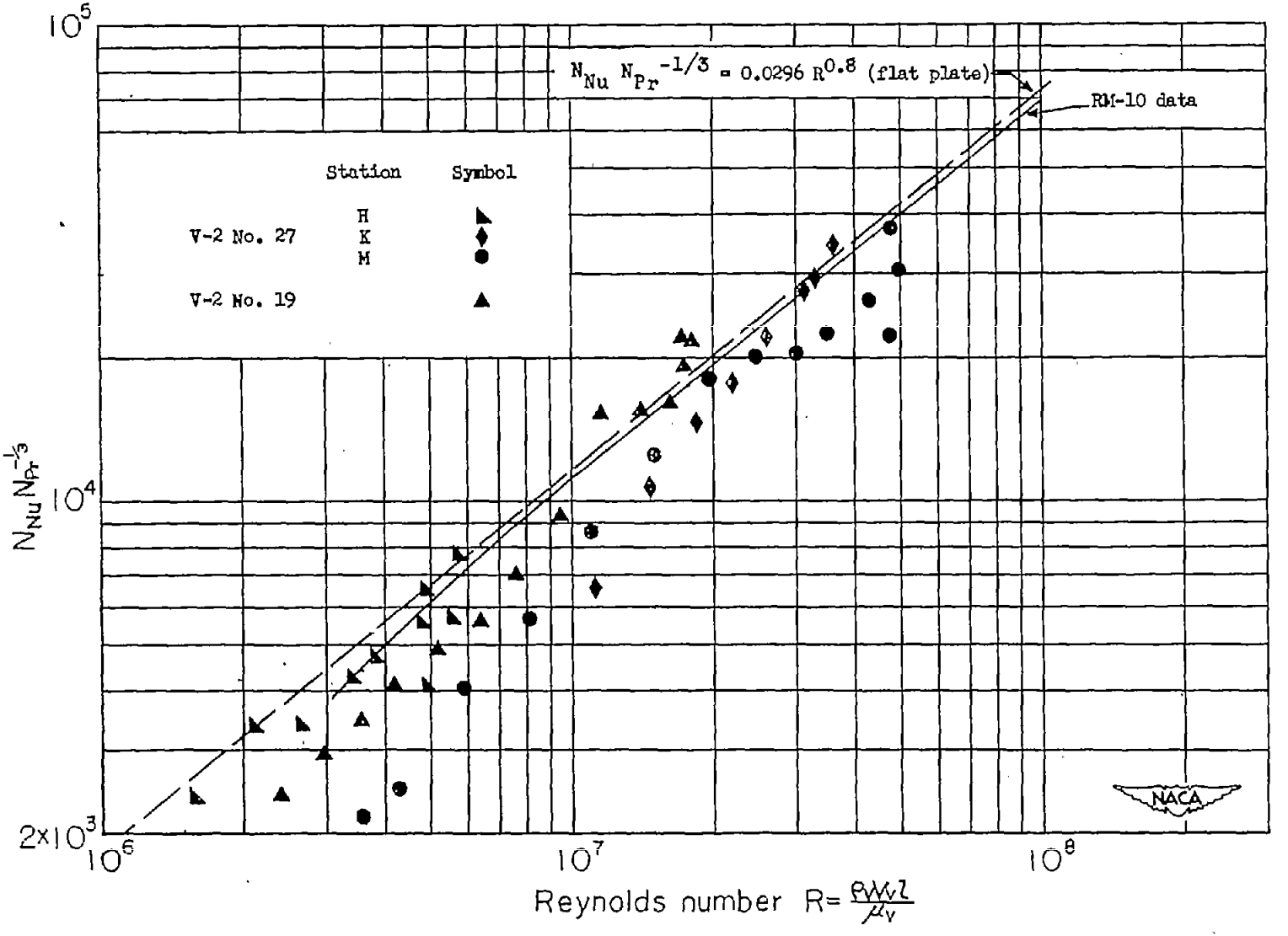


Figure 15.- Correlation of NACA RM-10 and V-2 heat-transfer data.

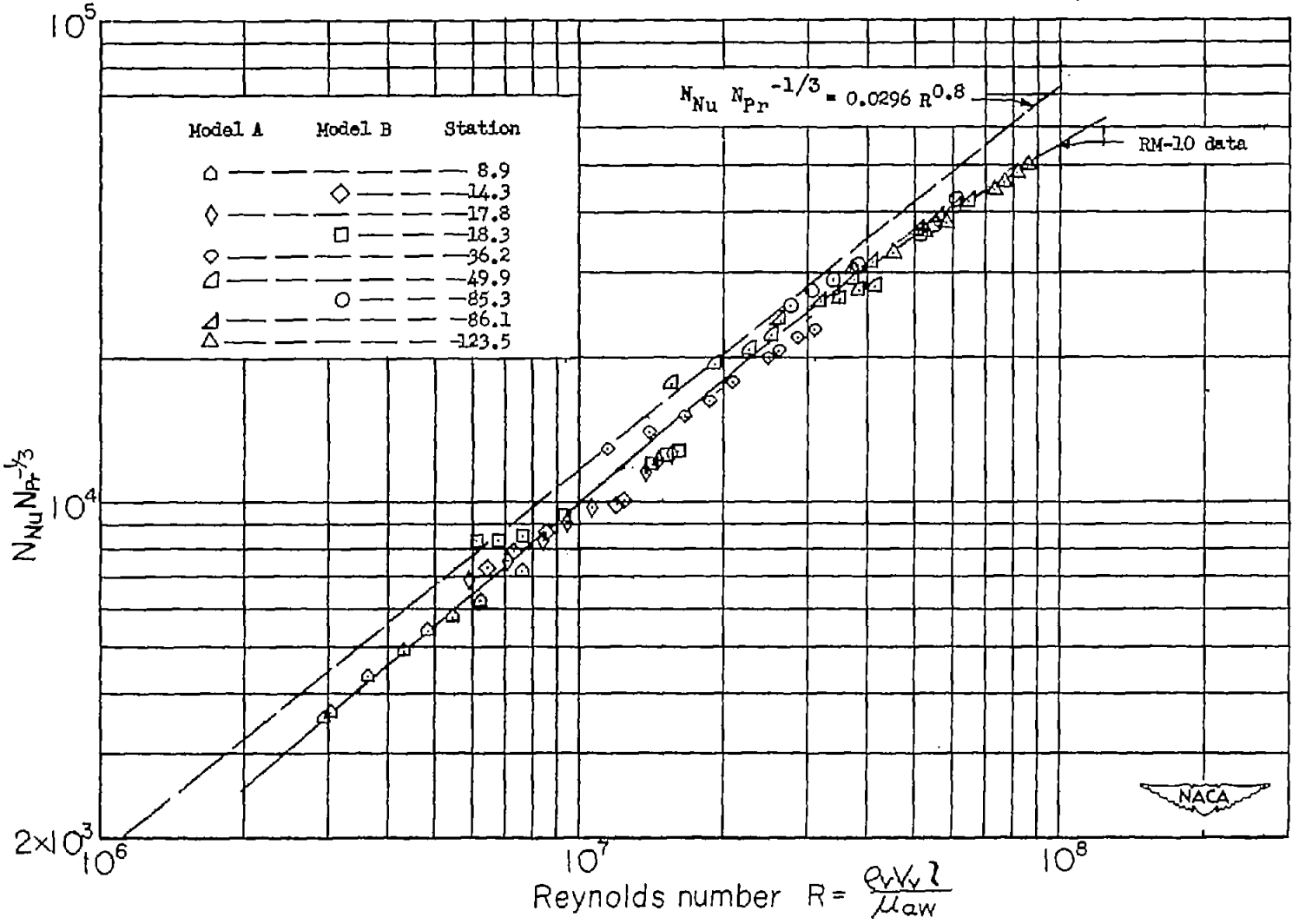


Figure 16.- Correlation of NACA RM-10 heat-transfer data (based on adiabatic wall temperature) with flat-plate formula.

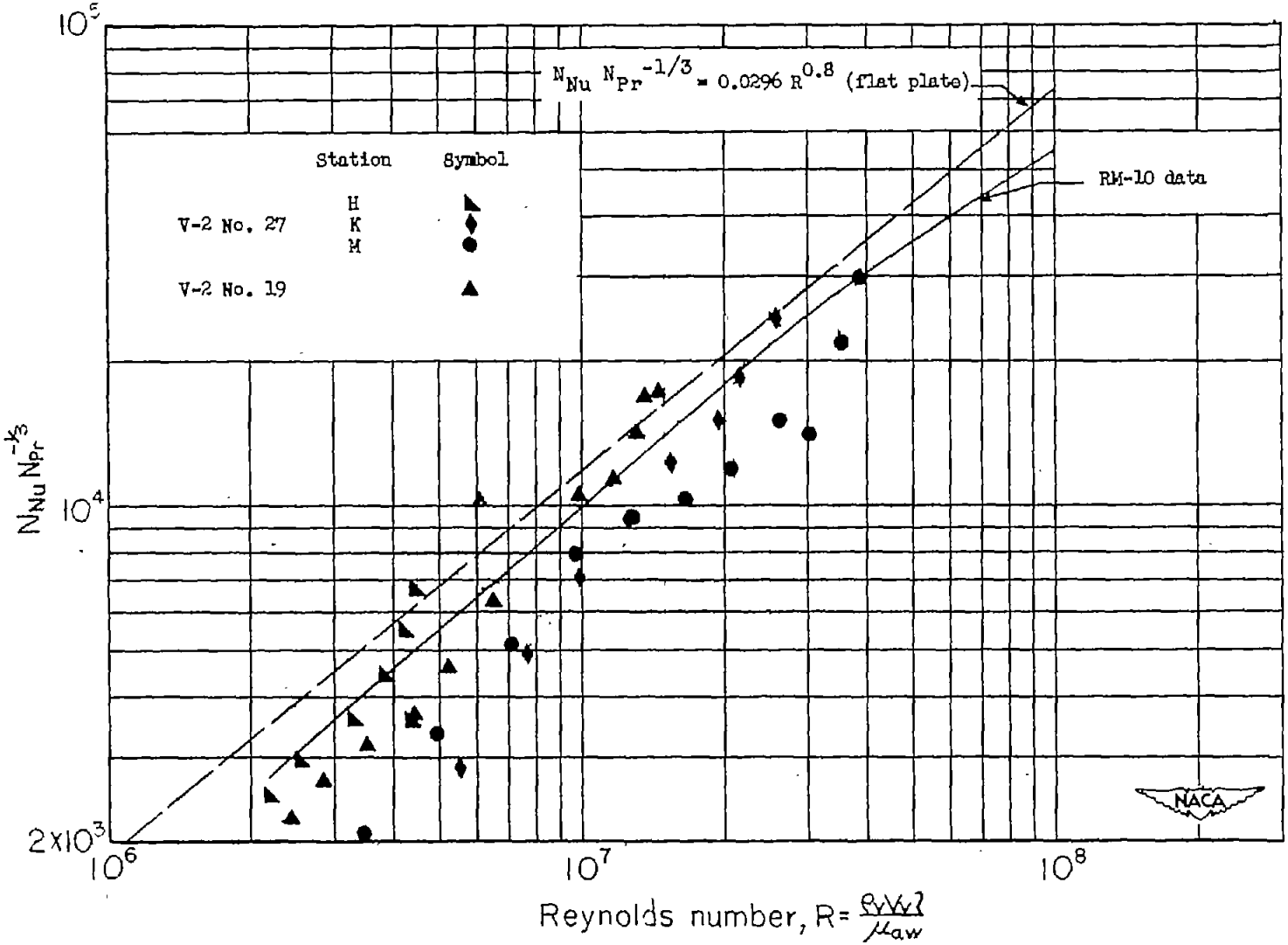


Figure 17.- Correlation of NACA RM-10 heat-transfer data (based on adiabatic wall temperature) with V-2 and flat-plate formula.

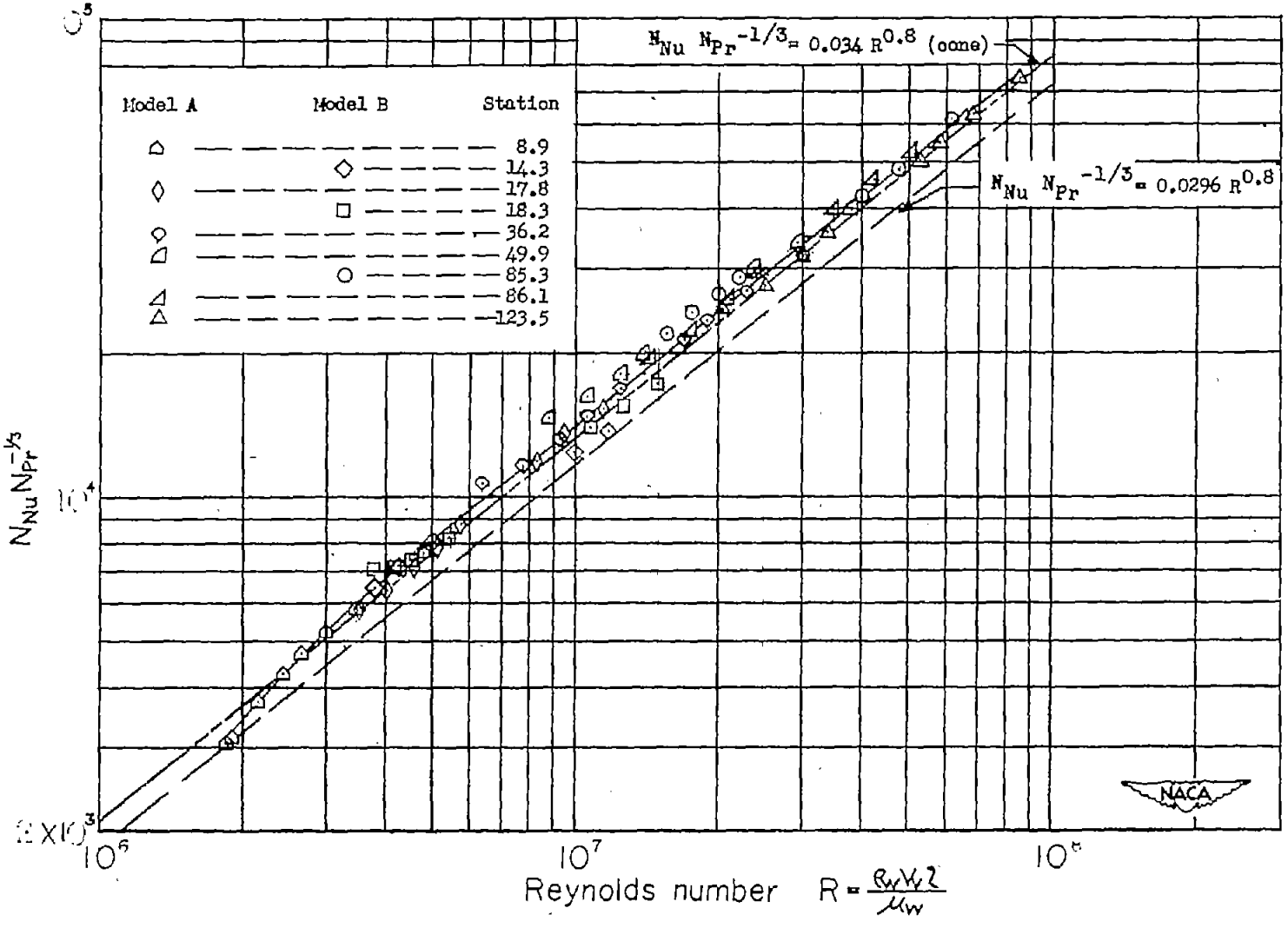


Figure 18.- Correlation of NACA RM-10 heat-transfer data (based on wall temperature) with turbulent flat-plate and cone formulas.

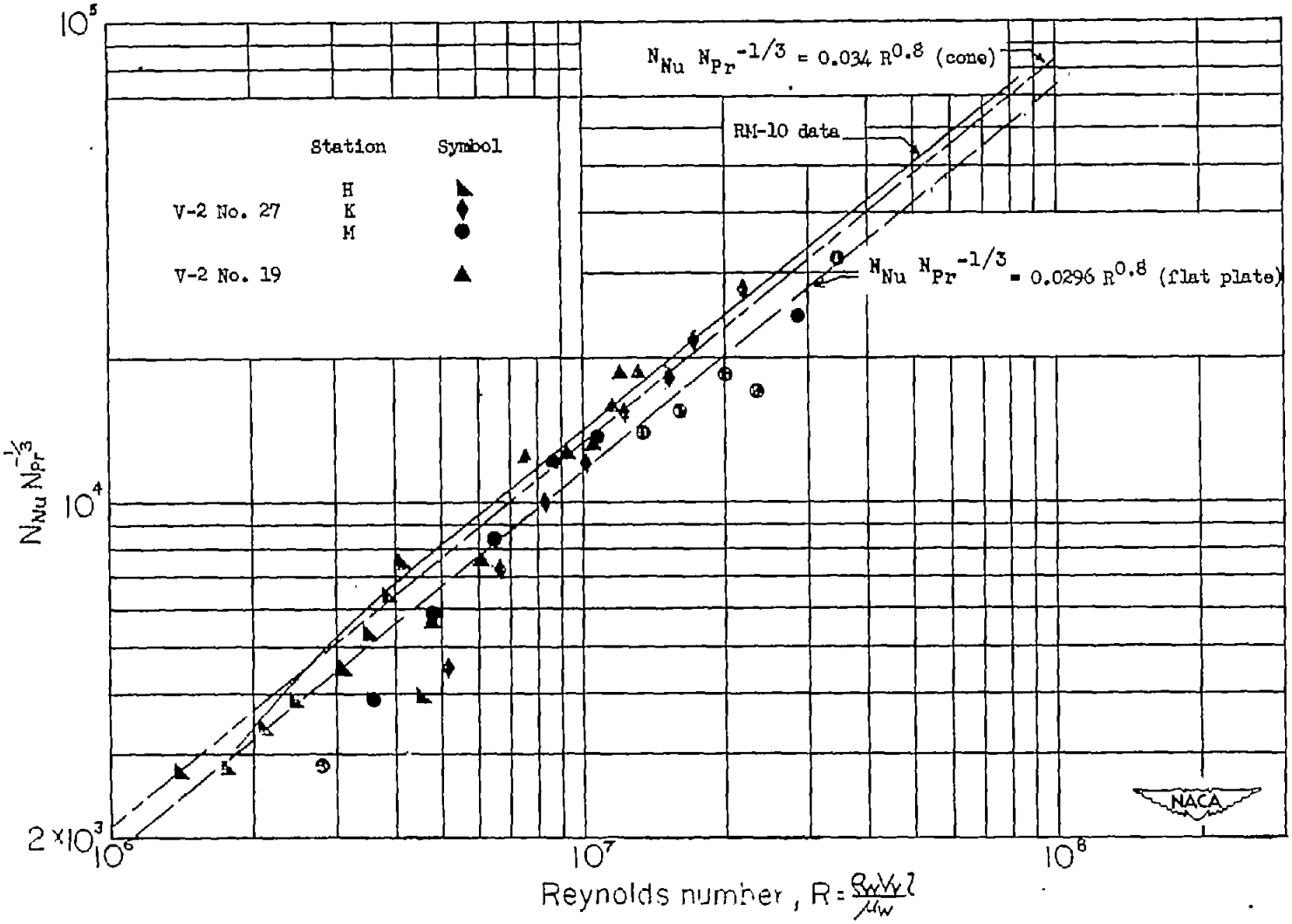


Figure 19.- Comparison of NACA RM-10 and V-2 heat-transfer data with turbulent flat-plate and cone formulas.